iScience, Volume *24*

Supplemental information

Ultrasensitive molecular building block for biothiol NMR detection at picomolar concentrations

Qingbin Zeng, Qianni Guo, Yaping Yuan, Baolong Wang, Meiju Sui, Xin Lou, Louis-S. Bouchard, and Xin Zhou

SUPPLEMENTAL INFORMATION

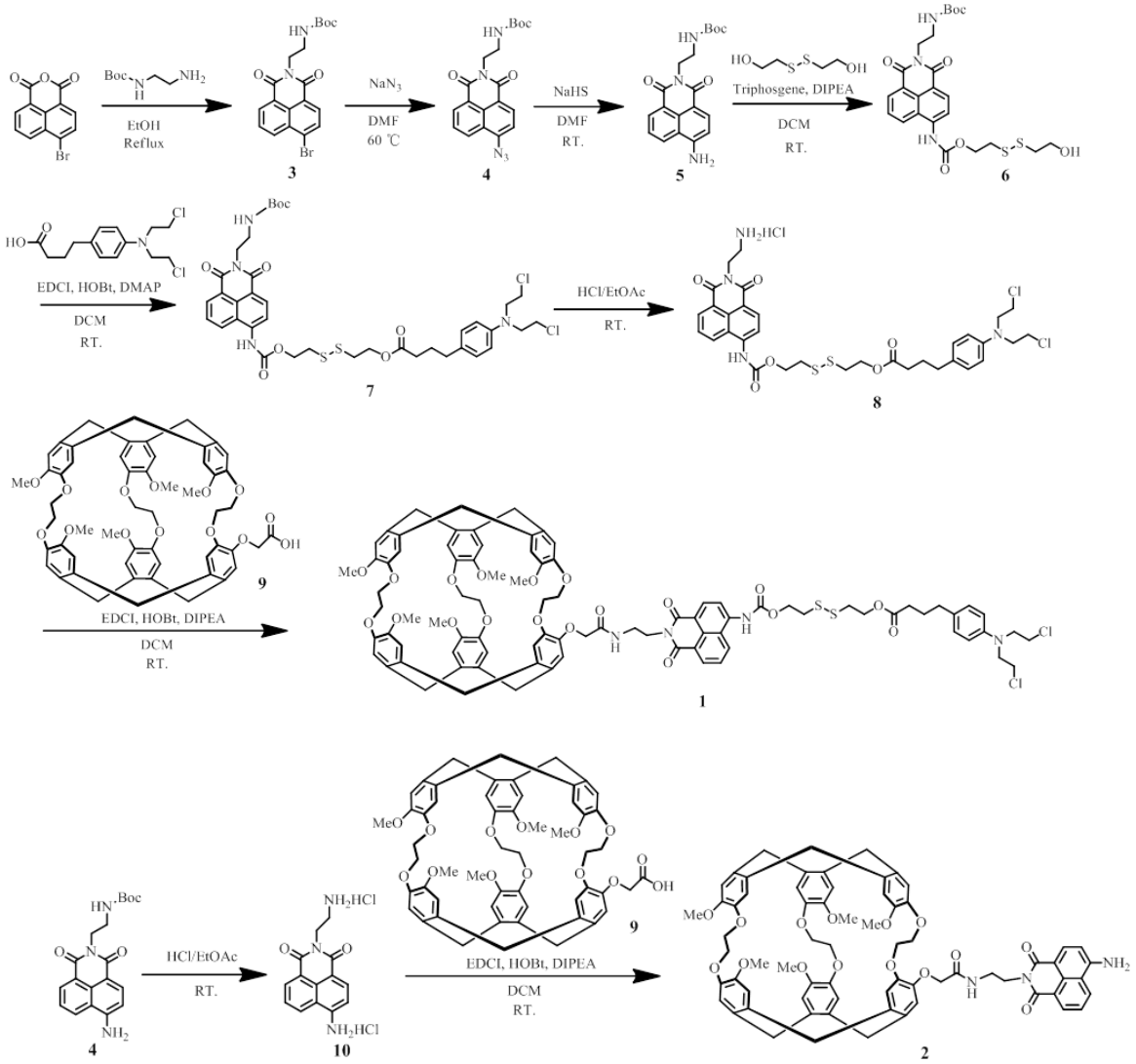

Scheme S1. Synthetic route of compound 1 and compound 2, Related to STAR Methods.

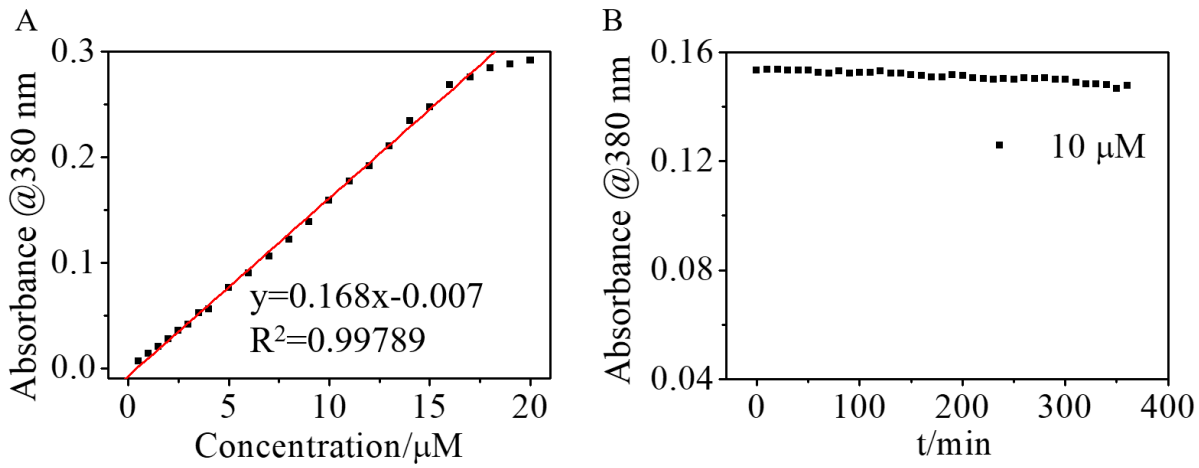

Figure S1. Absorption spectra of Molego 1 in solution, Related to STAR Methods. (A) Concentration dependent and (B) time dependent absorption of Molego **1** at 380 nm. The absorption of **1** at 380 nm was linear at low concentration while showing nonlinear behavior at higher concentrations. All spectra were acquired at room temperature in PBS buffer (pH=7.4, including 50% DMSO).

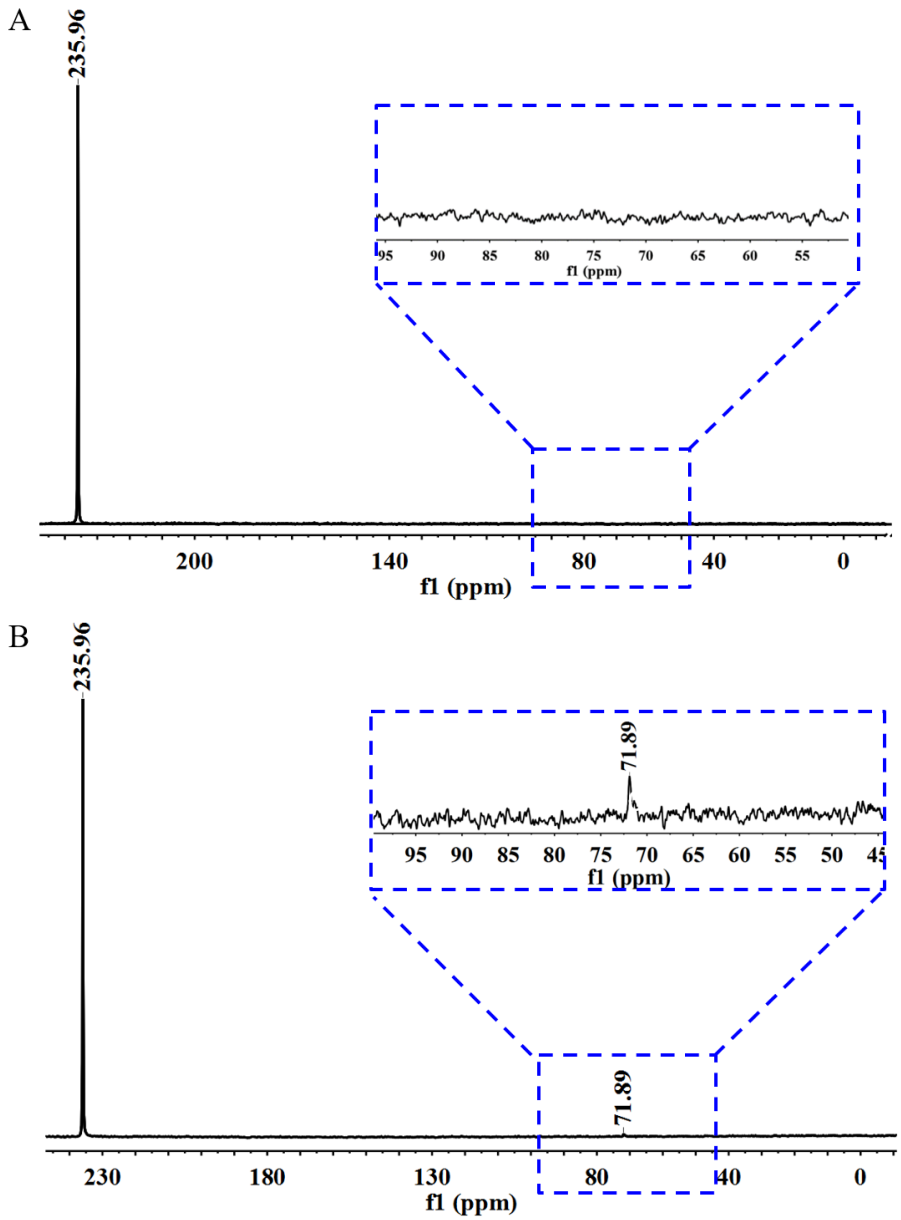

Figure S2. Hyperpolarized ^{129}Xe NMR spectra for the Molego 1 (25 μM) before and after reacted with biothiols, Related to STAR Methods. (A) Before the Molego **1** reacted with GSH (NS=16, LB=5 Hz), (B) After the Molego **1** reacted with GSH (500 equiv) for 3 h at 37 °C (NS=16, LB=5 Hz). The spectra were acquired at room temperature in PBS buffer (pH=7.4, 20 mM), containing 50% DMSO (v/v).

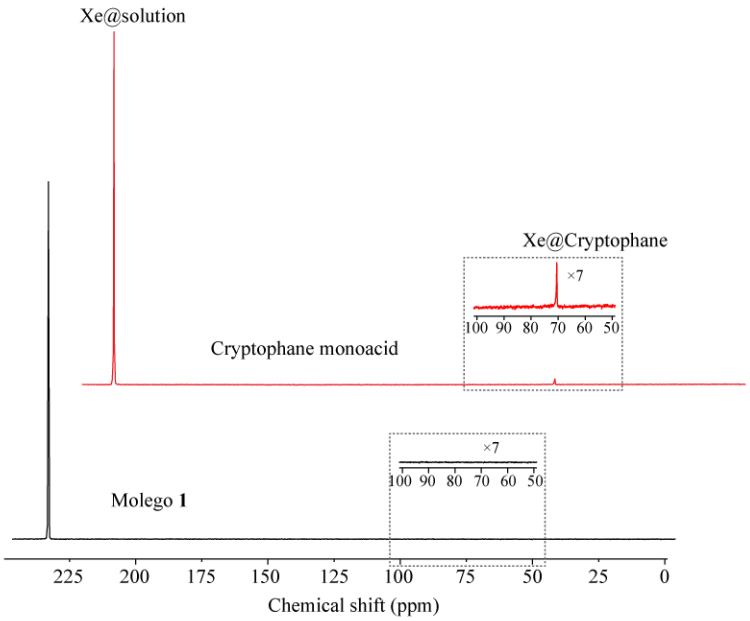

Figure S3. **Hyperpolarized ^{129}Xe NMR of Molego 1 (25 µM) and cryptophane-A mono acid (25 µM), Related to STAR Methods.** The spectra were acquired at room temperature in PBS buffer (pH=7.4, 20 mM), containing 50% DMSO (v/v). (NS=32, LB=5 Hz).

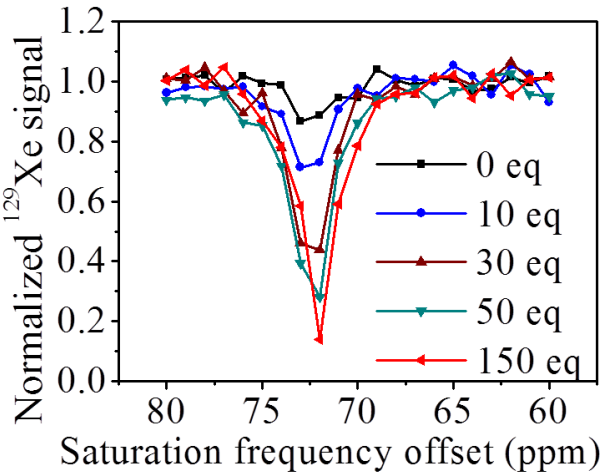

Figure S4. Hyper-CEST spectra of Molego 1 (5 μM) response to different concentrations of GSH, Related to Figure 2. All spectra were acquired at room temperature after incubation at 37 °C for 3 h in PBS buffer (pH=7.4, 20 mM), including 50% DMSO (v/v).

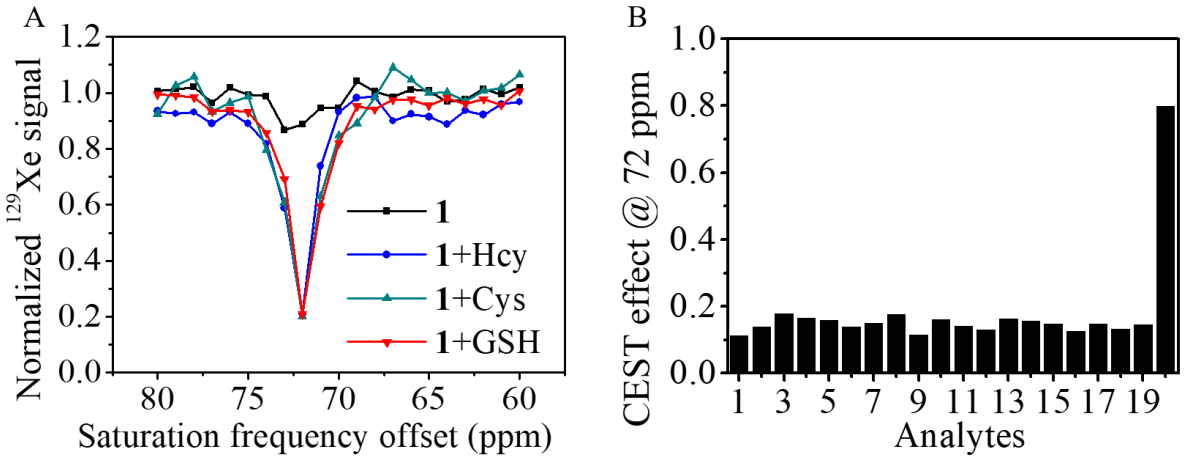

Figure S5. Hyper-CEST spectra of Molego 1 (5 μM) response to different analytes, Related to Figure 2. (A) Hyper-CEST spectra of **1** response to biothiols (GSH, Hcy, Cys). (B) Hyper-CEST at 72 ppm of **1** response to nonthiol amino acids (1, only biosensor; 2, Val; 3, Leu; 4, Ile; 5, Phe; 6, Trp; 7, Met; 8, Pro; 9, Gly; 10, Ser; 11, Thr; 12, Tyr; 13, Asn; 14, Gln; 15, His; 16, Lys; 17, Arg; 18, Asp; 19, Glu; 20, Ala; 21, GSH). The concentrations of biothiols, nonthiol amino acids were kept at 1 mM. All spectra were acquired at room temperature after incubation at 37 °C for 3 h in PBS buffer (pH=7.4, 20 mM), including 50% DMSO (v/v).

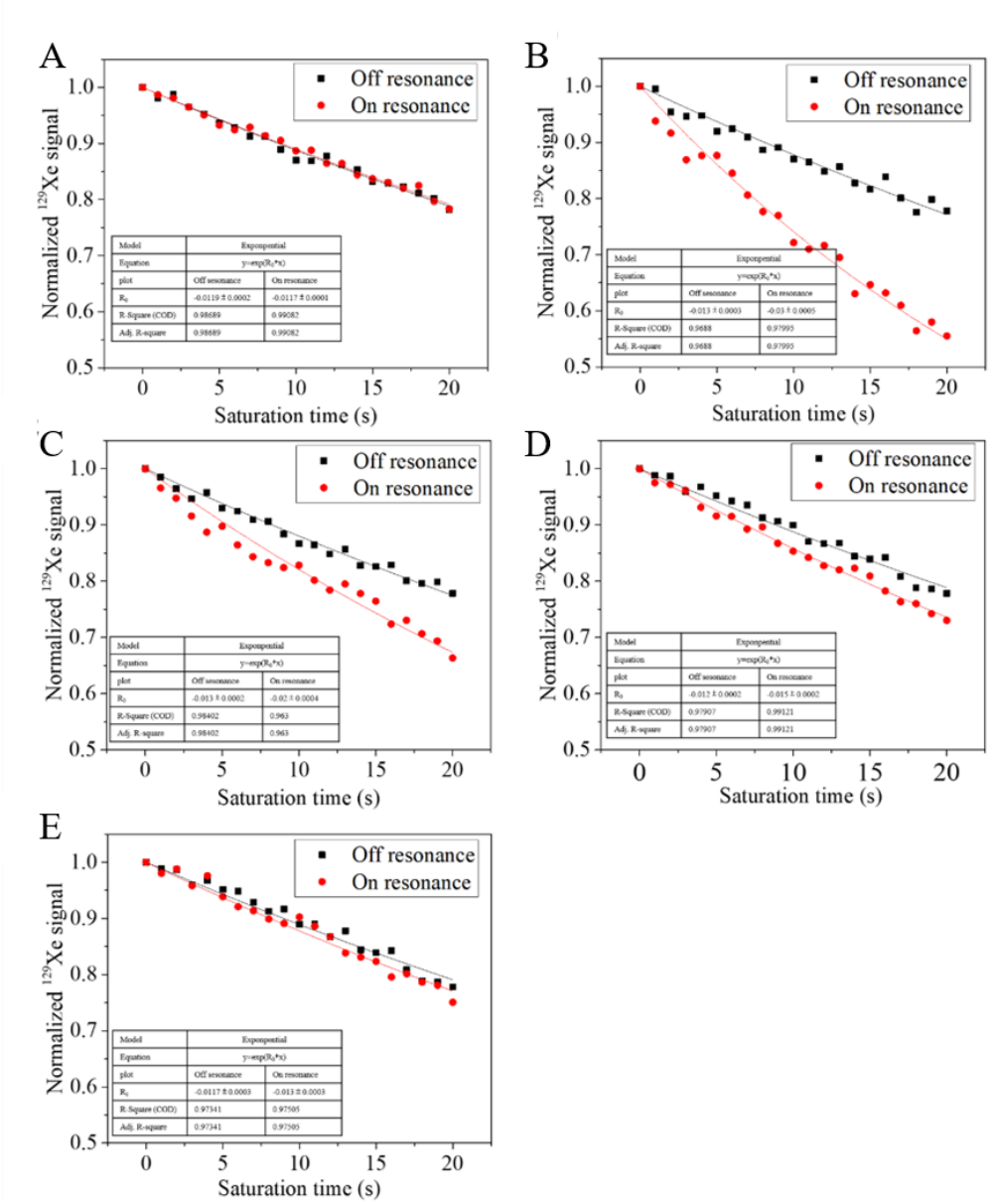

Figure S6. Saturation profiles of different concentration Molego 1, Related to STAR Methods. (A) 20 mM PBS (including 50% DMSO). (B) 500 nM **1**. (C) 10 nM **1**. (D) 200 pM **1**. (E) 100 pM **1**. All spectra were acquired at room temperature after the Molego **1** reacted with GSH (100 equiv) in PBS buffer (pH=7.4, 20 mM), including 50% DMSO (v/v). All samples were saturated by a cw-saturation pulse with a 13 μT field. Saturation frequencies of cw pulses were positioned +164 ppm and -164 ppm referenced to Xe-aq peak, for off- and on-resonance. Each saturation profile was fit to an exponential decay equation [f(t) = exp(-t/τ)].

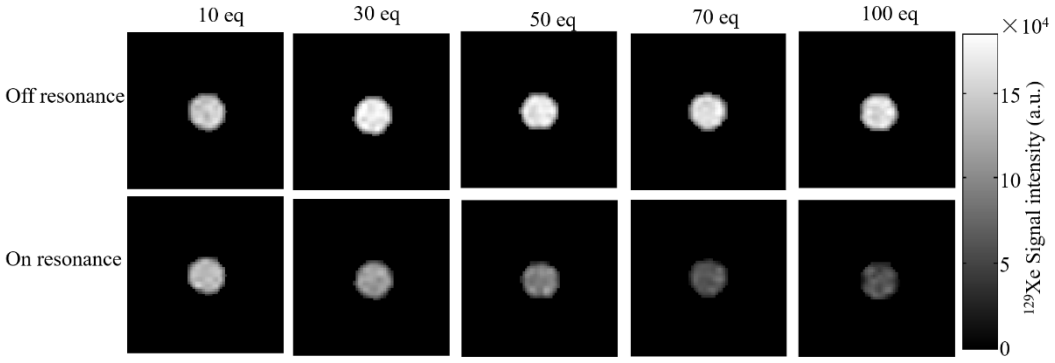

Figure S7. Hyperpolarized ^{129}Xe MRI for Molego 1 (5 μM) response to different concentration of GSH, Related to Figure 2. All images were acquired at room temperature after the Molego **1** reacted with different concentration of GSH in PBS buffer (pH=7.4, 20 mM), including 50% DMSO (v/v).

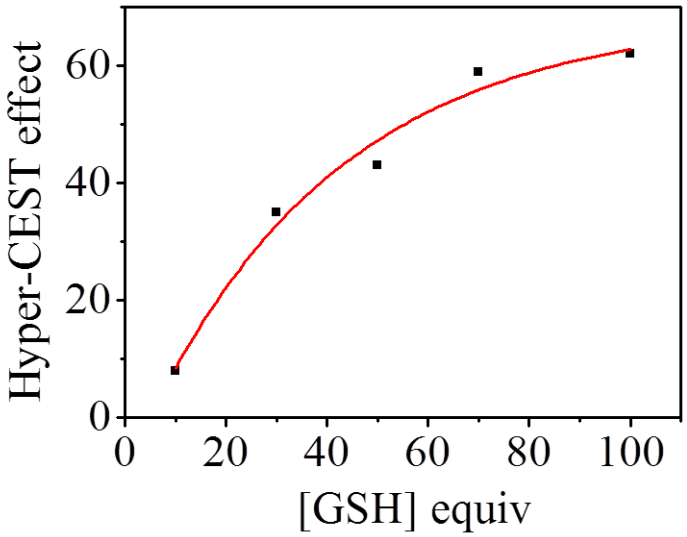

Figure S8. The average Hyper-CEST effect of Molego 1 (5 μM) reacted with different concentration of GSH (containing 50% DMSO), Related to Figure 2. The Hyper-CEST effect was calculated based on the average of 4 on-resonant (saturation on Xe @ cage: -164 ppm) and 4 off-resonant (saturation at 164 ppm) images (The chemical shift of dissolved ^{129}Xe was set as 0 ppm).

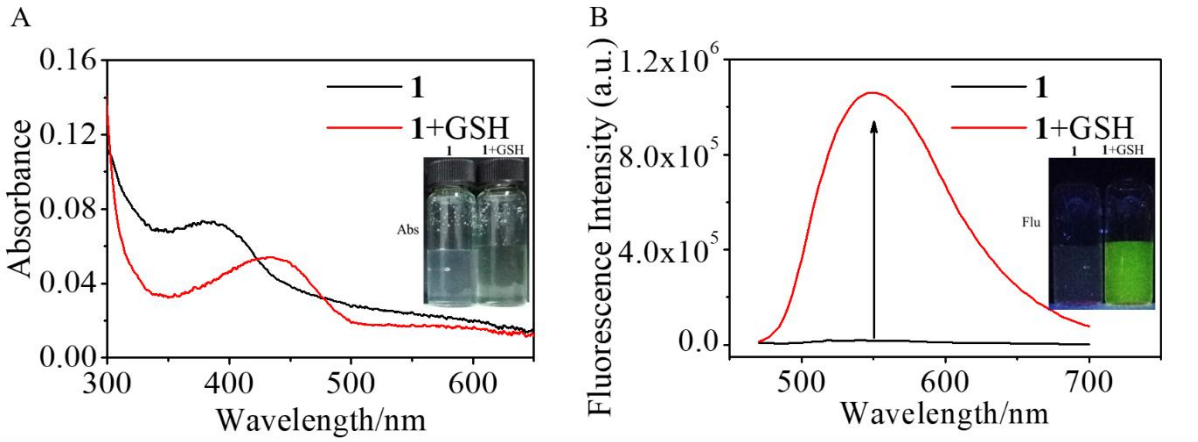

Figure S9. Optical spectroscopic studies of Molego 1 (5 μM) in aqueous solution, Related to STAR Methods. (A) Absorption spectra of **1** (black line, in the absence of GSH; red line, in the presence of GSH). (B) Fluorescence spectra of **1** (black line, in the absence of GSH; red line, in the presence of GSH). All spectra and photographs were obtained at room temperature after **1** was allowed to incubate with amino acid at 37 °C for 3 h in buffer (containing 50% DMSO).

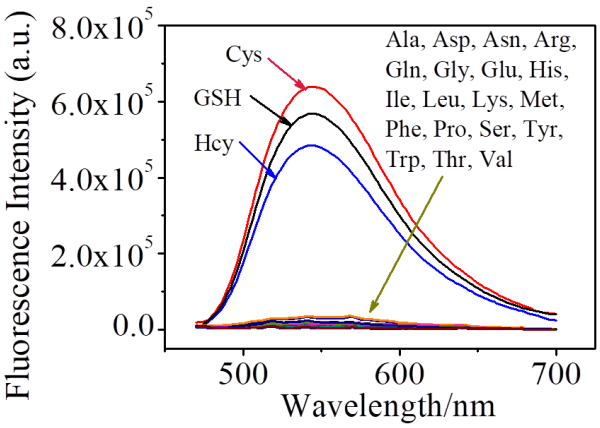

Figure S10. **Fluorescence response of Molego 1 for biothiols and nonthiol amino acids, Related to STAR Methods.** The concentration of nonthiol amino acids, biothiols were kept at 500 μM. All spectra were obtained at room temperature after Molego **1** was incubated with amino acid at 37 °C for 3 h in buffer (pH 7.4, containing 50% DMSO).

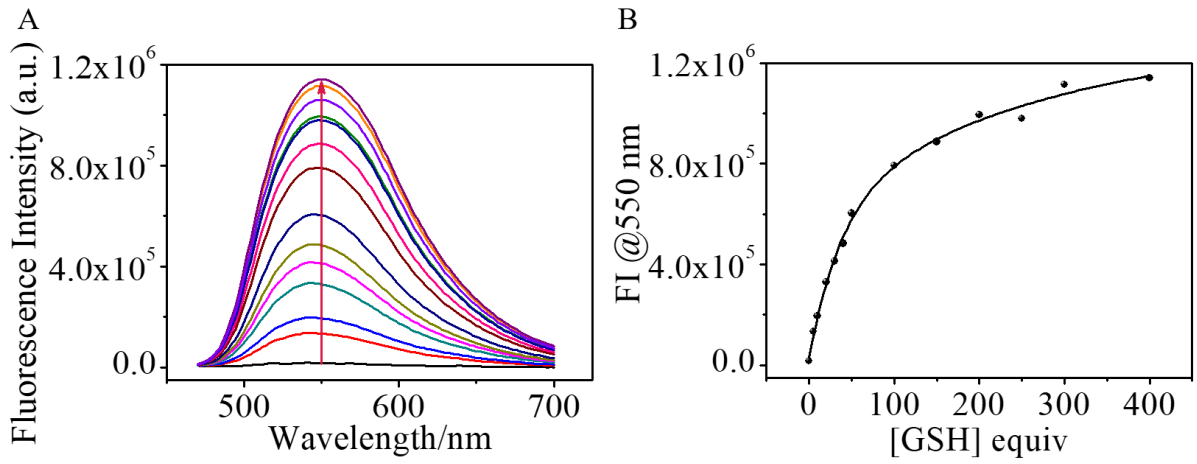

Figure S11. Fluorescence spectra of Molego 1 after reacted with different concentrations of GSH, Related to STAR Methods. (A) Fluorescence response of Molego **1** (5 μM) for different concentrations of GSH. (B) Change in fluorescence intensity at 550 nm as a function of GSH concentration. All spectra were acquired at room temperature after incubation at 37 °C for 3 h in PBS buffer (pH=7.4, including 50% DMSO).

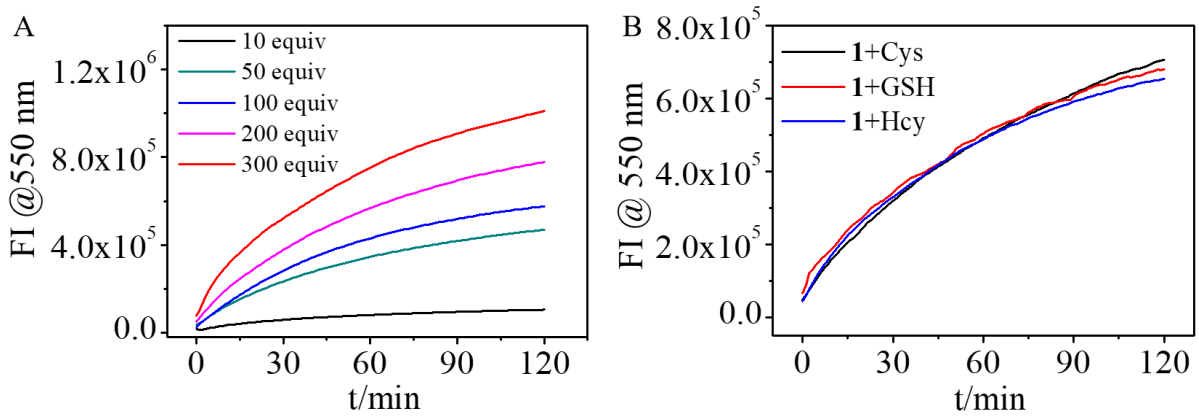

Figure S12. Kinetic scan of Molego 1 (5 μM) treated by different concentrations of GSH and different biothiols, Related to STAR Methods. (A) Fluorescence response of **1** for different concentrations of GSH. (B) Fluorescence response of **1** for GSH, Cys, and Hcy. The concentration of biothiols kept at 500 μM. All spectra were acquired at 37 °C in PBS buffer (pH 7.4, including 50% DMSO).

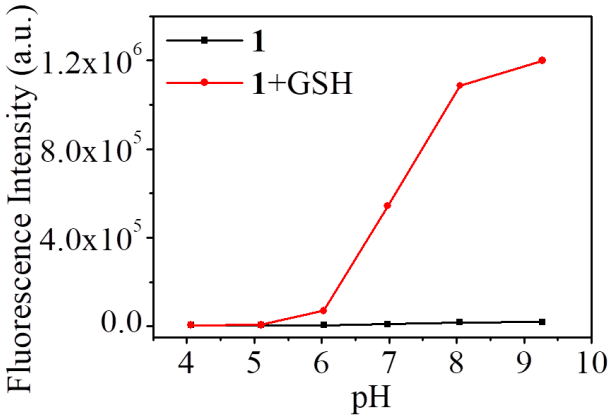

Figure S13. **Fluorescence response of Molego 1 with and without GSH as a function of pH, Related to STAR Methods.** All spectra were obtained at room temperature after Molego **1** was incubated with GSH at 37 °C for 3 h in different pH buffer (containing 50% DMSO).

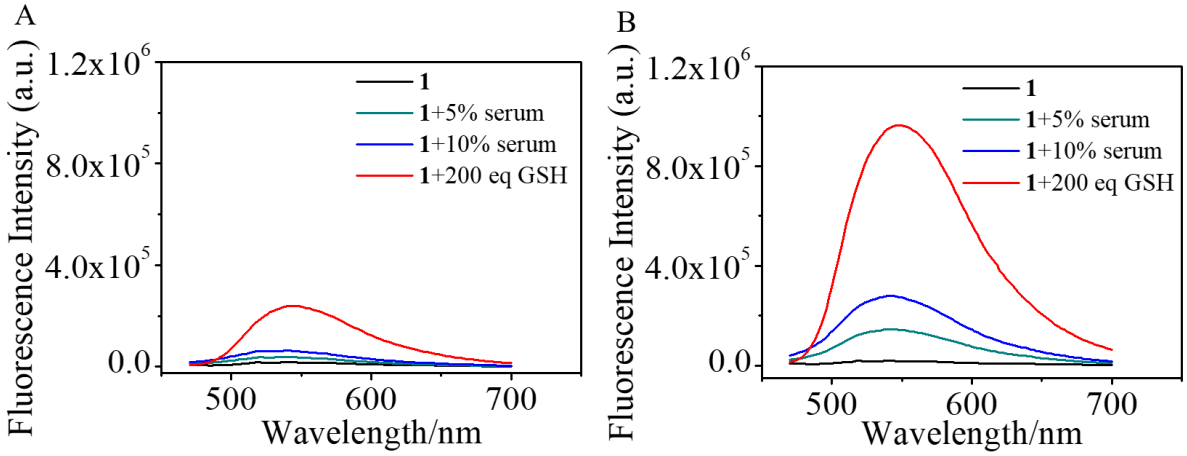

Figure S14. Fluorescence response of Molego 1 (5 μM) for biothiols and serum, Related to STAR Methods. (A) After the biothiols and serum reacted with the Molego **1** for 3 h at room temperature. (B) After the biothiols and serum.

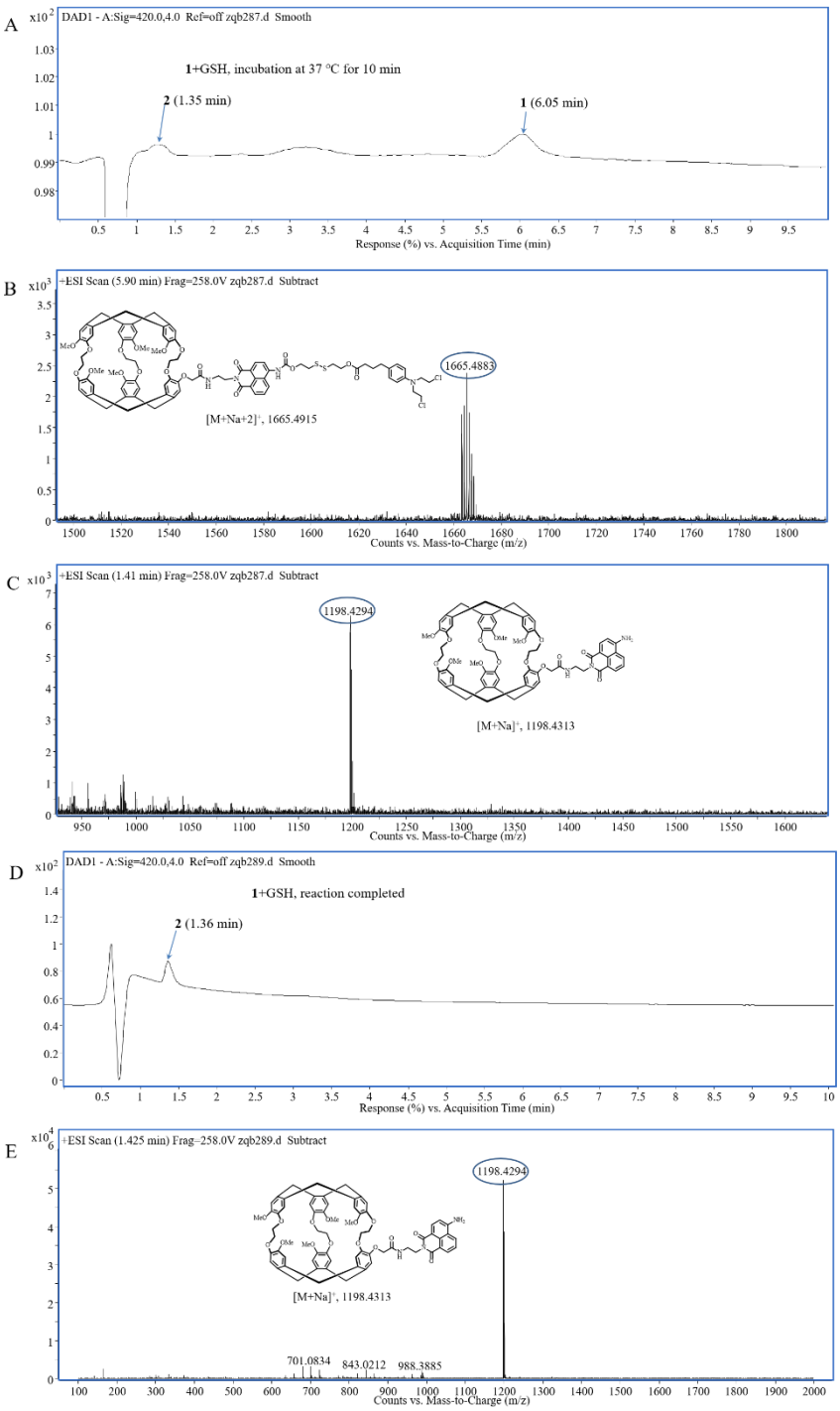

Figure S15. LC-MS analysis of Molego 1 reaction with GSH, Related to STAR Methods. (A) LC analysis of Molego **1** after reacted with GSH for 10 min. (B) and (C) MS analysis of Molego **1** after reacted with GSH for 10 min. (D) LC analysis of Molego **1** after reacted with GSH completed. (E) MS analysis of Molego **1** after reacted with GSH completed. Peaks in the chromatograms were detected by monitoring the UV/Vis absorption at 420 nm.

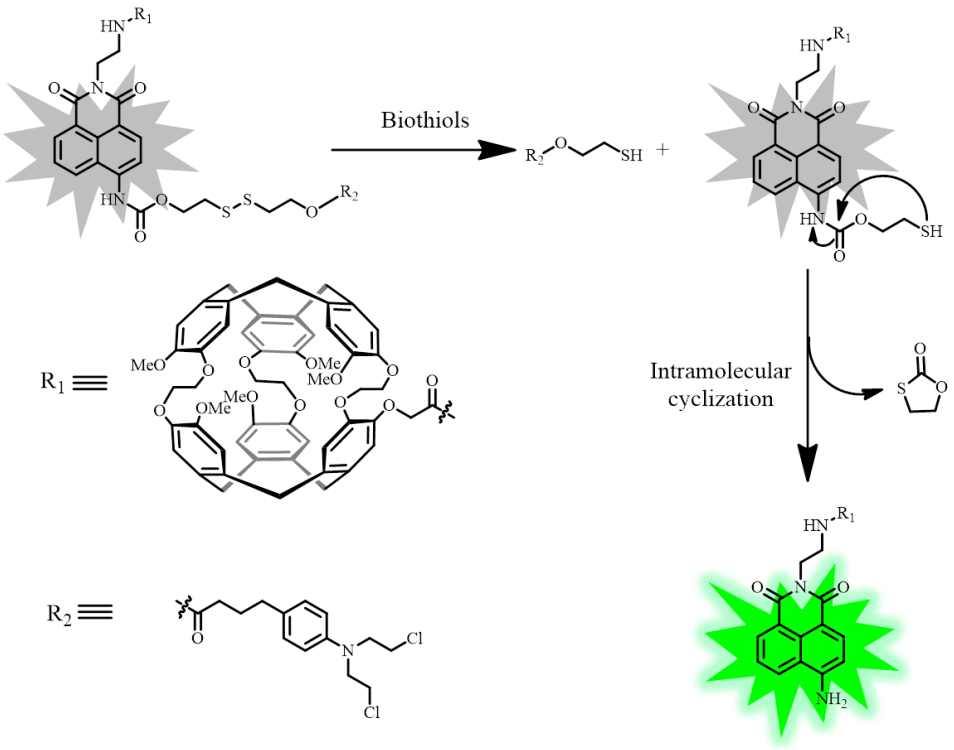

Scheme S2. **Proposed mechanism of Molego 1 reaction with biothiols, Related to STAR Methods.** Before the Molego **1** reacted with biothiols, the fluorescence signal of Molego **1** was silent. After the disulfide bond of Molego **1** was cleaved by GSH, an intramolecular cyclization followed, which leads to the activation of the fluorescent moiety.

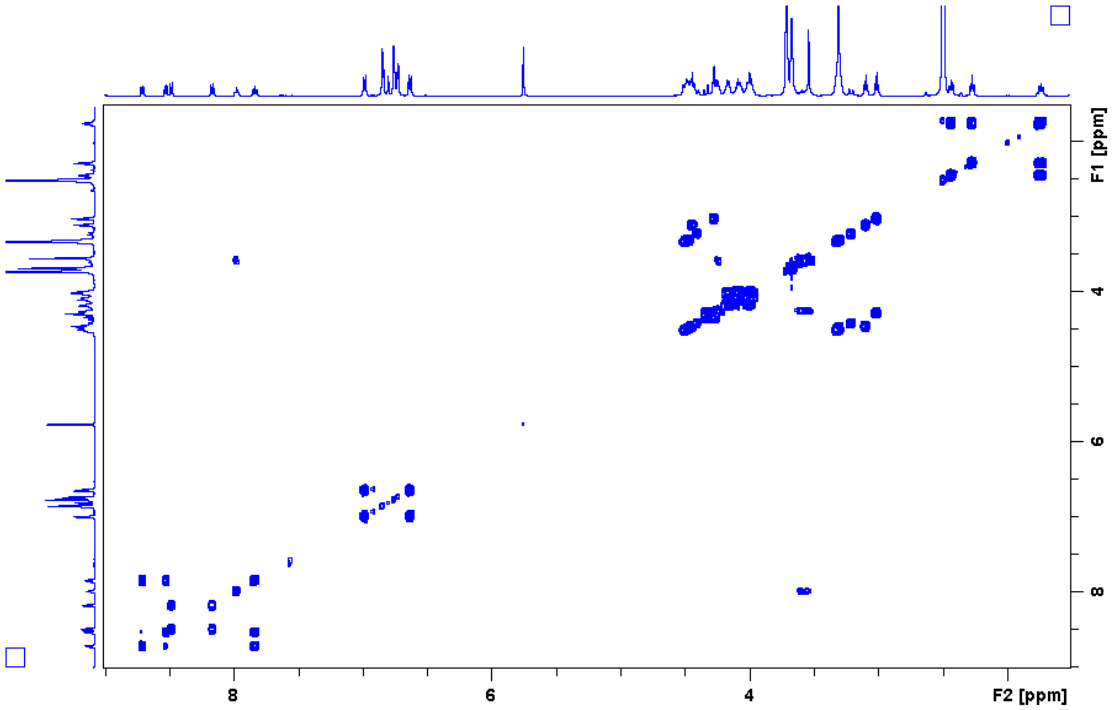

Figure S16. ^{1}H-^{1}H COSY of Molego 1 (4 mM) in DMSO-d6, Related to Figure 3. The experiments were performed at 298 K on a Bruker Avance III 500 NMR instrument equipped with a triple resonance clamp probe.

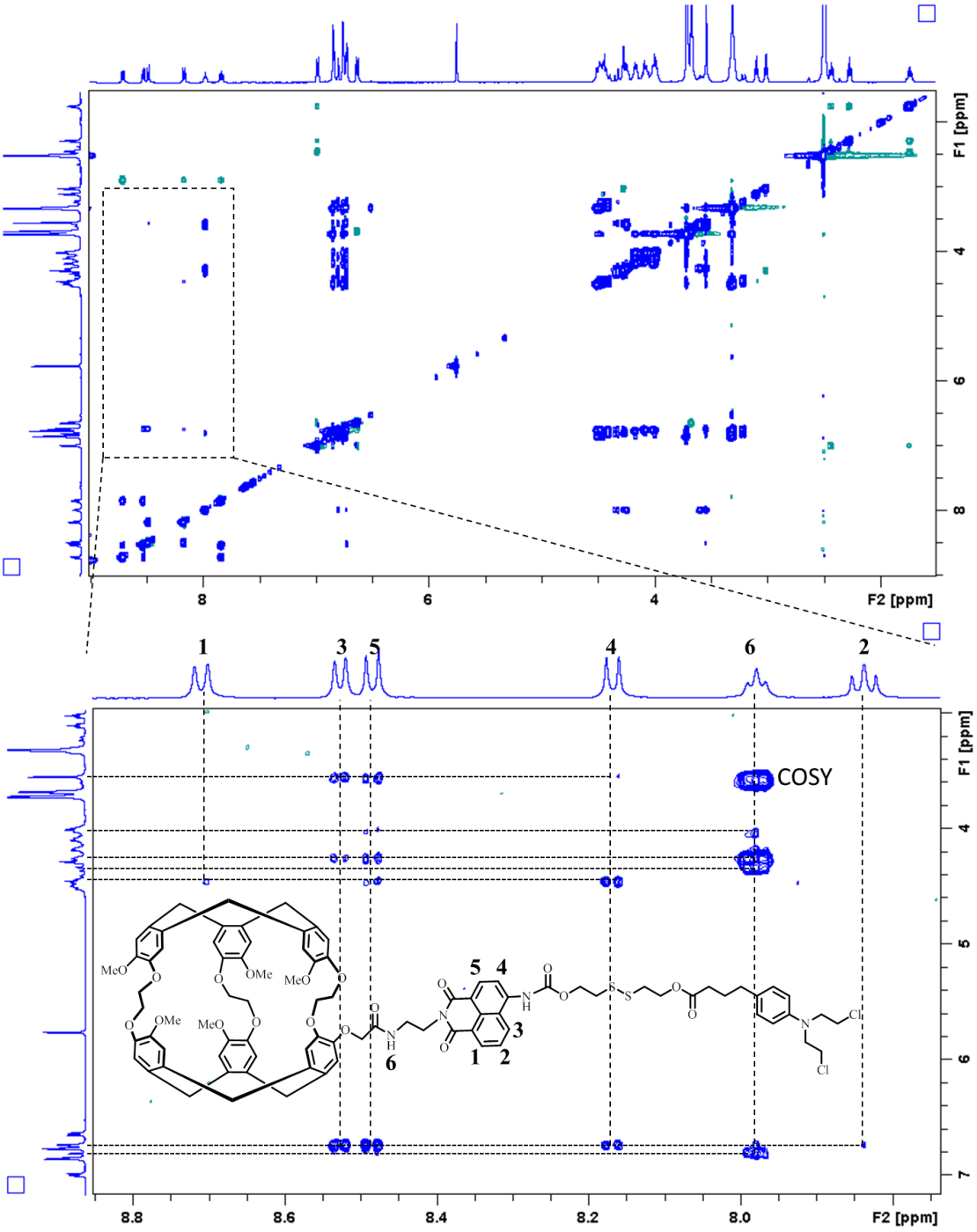

Figure S17. ^{1}H-^{1}H NOESY of Molego 1 (4 mM) in DMSO-d6, Related to Figure 3. The experiments were performed at 298 K on a Bruker Avance III 500 NMR instrument equipped with a triple resonance clamp probe. The mixing time for magnetization transfer by cross-relaxation was 1500 ms.

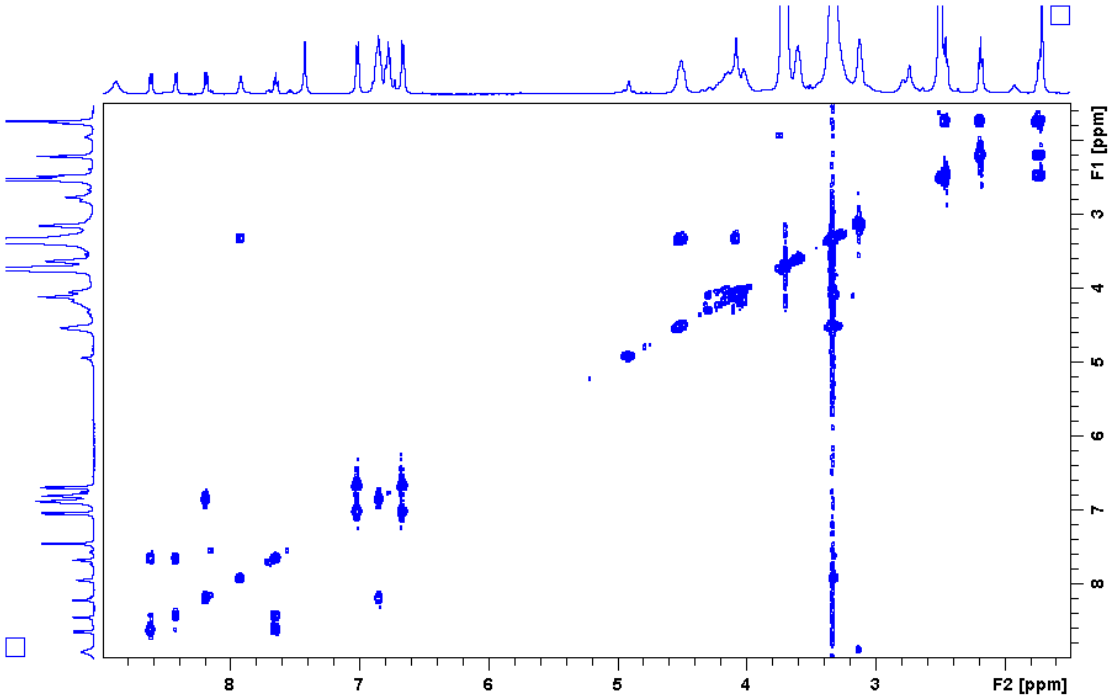

Figure S18. ^{1}H-^{1}H COSY of compound 2 (4 mM) and chlorambucil in DMSO-d6, Related to Figure 3. The experiments were performed at 298 K on a Bruker Avance III 500 NMR instrument equipped with a triple resonance clamp probe.

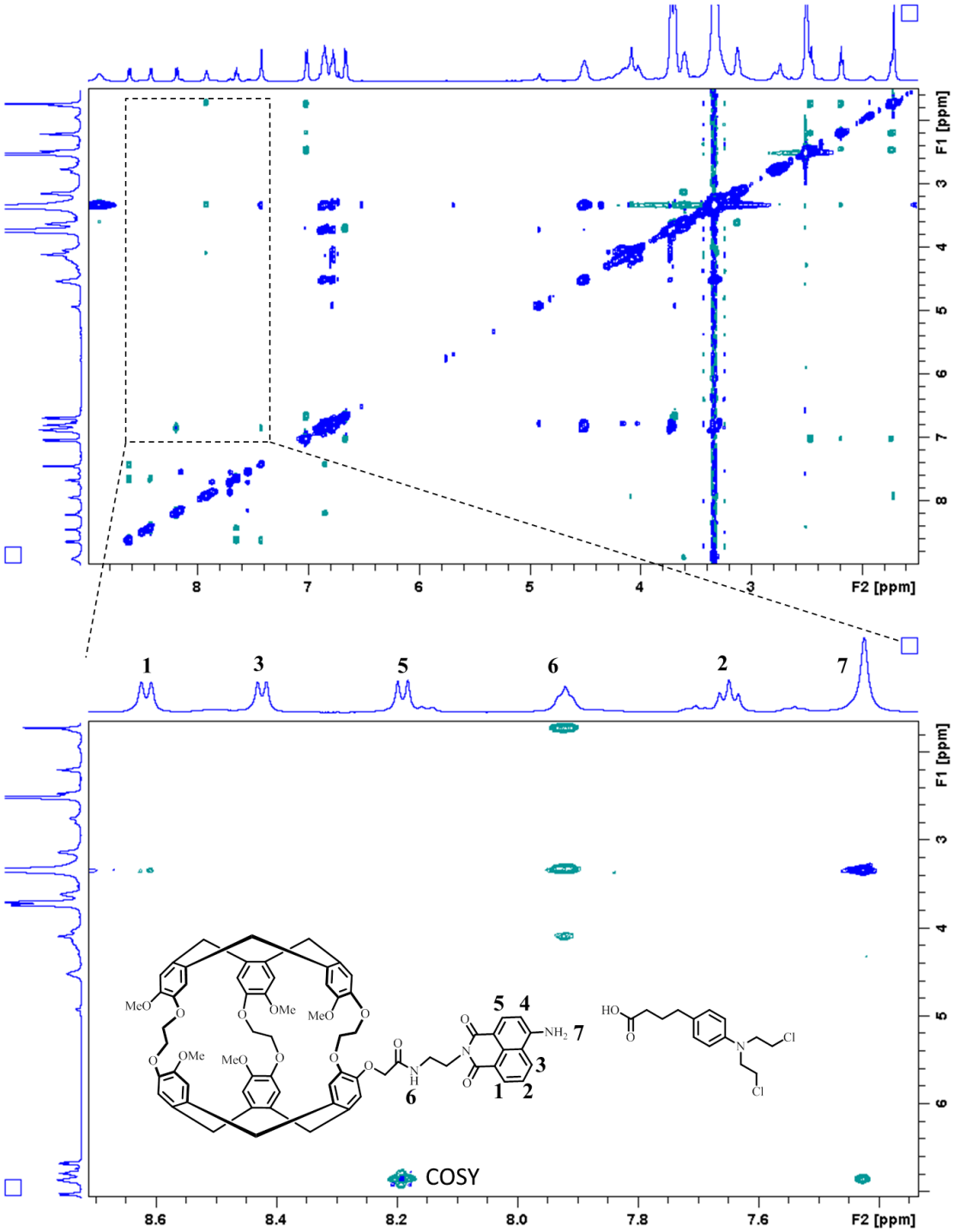

Figure S19. ^{1}H-^{1}H NOESY of compound 2 (4 mM) and chlorambucil in DMSO-d6, Related to Figure 3. The experiments were performed at 298 K on a Bruker Avance III 500 NMR instrument equipped with a triple resonance clamp probe. The mixing time for magnetization transfer by cross-relaxation was 1500 ms.

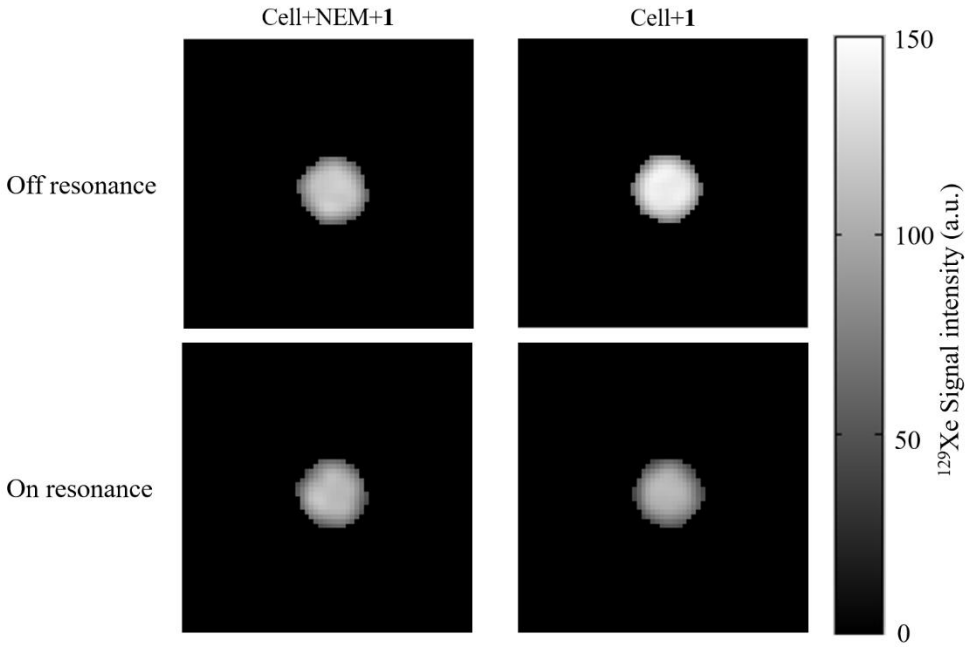

Figure S20. Hyperpolarized ^{129}Xe MRI for Molego 1 (30 μM) response to GSH in cells, Related to Figure 5.

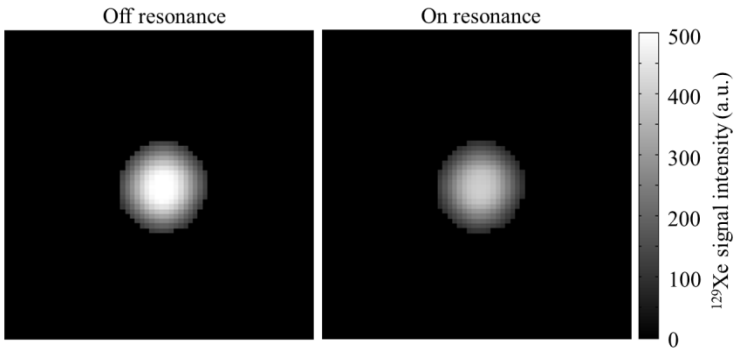

Figure S21. Hyperpolarized ^{129}Xe MRI for A549 tumor lysate with Molego 1, Related to Figure 5. The tumor was resected after the A549 tumor model mice was injected with Molego **1** (1 mM, in 100 μL of PBS solution, including 1% DMSO, 1% Cremophor®EL)) through intratumor injection, and then the tumor was make of homogenate through homogenizing machine. Finally, the Hyper-CEST spectrum was obtained.

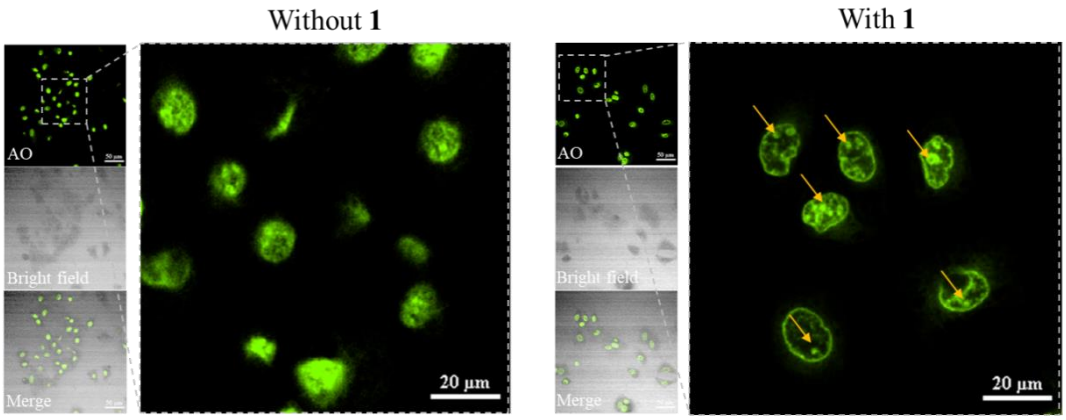

Figure S22. **CLSM images of AO-stained A549 cells incubated with or without Molego 1 for 4 h, Related to STAR Methods.** Yellow arrows indicate the apoptotic body in nuclear. The scale bar represents 20 μm or 50 μm.

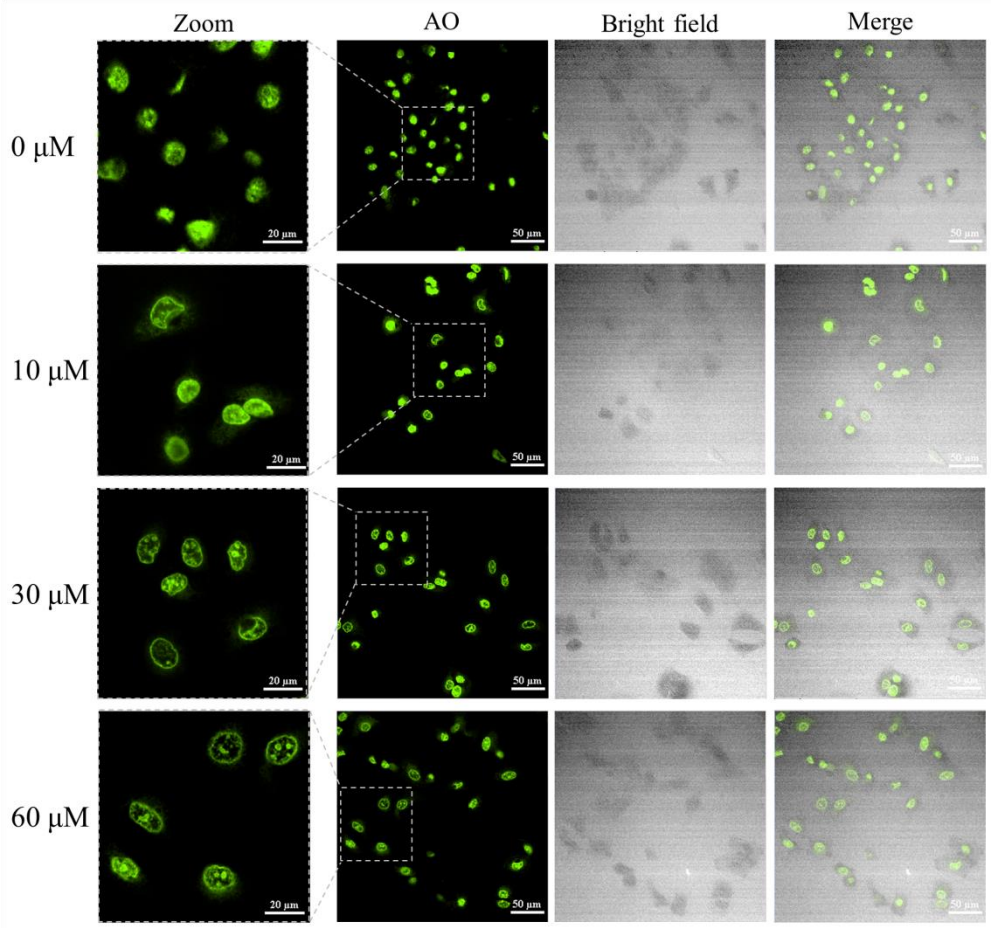

Figure S23. CLSM images of AO-stained A549 cells incubated with different concentration of Molego 1 (0 μM, 10 μM, 30 μM, 60 μM) for 4 h, Related to STAR Methods. The quantity of spotty green or granular core cells increased with the concentration of Molego **1** increased. The scale bar represents 20 μm or 50 μm.

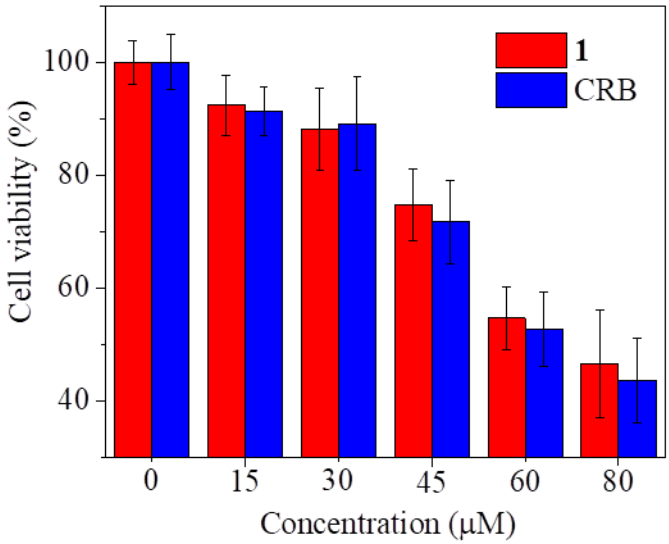

Figure S24. Cell viability of A549 cells after treatment with Molego 1 and CRB at different concentrations for 48 h, Related to STAR Methods.

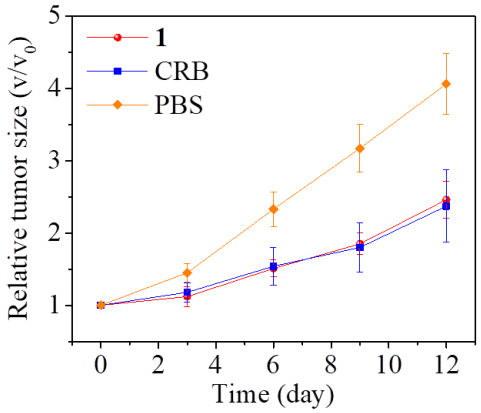

Figure S25. Relative tumor growth curves of A549 tumor-bearing mice with various treatments, Related to STAR Methods (the data are shown as mean ± SD (n= 4). The Molego **1** group exhibited obviously tumor growth inhibition than the PBS group, and kept consistent with CRB group

Figure S26. **Photograph of tumor excised from mice after different treatments, Related to STAR Methods.**

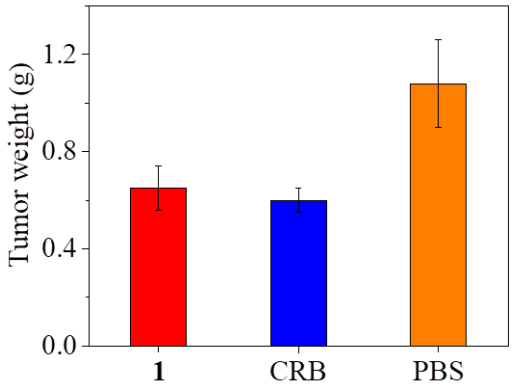

Figure S27. Mice tumor weight curves with different treatments, Related to STAR Methods. Error bars are based on the standard deviations (SD) of 4 mice.

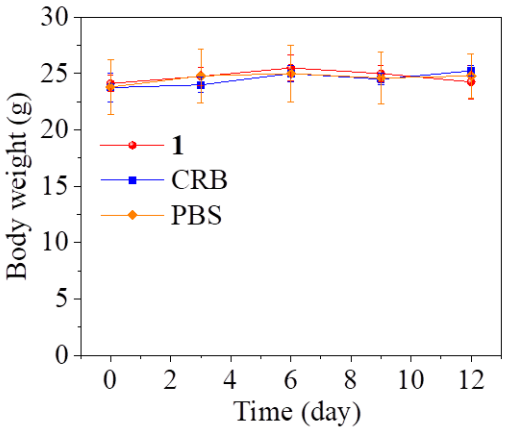

Figure S28. Mice body weight curves with relevant treatments, Related to STAR Methods. All groups did not exhibit body weight loss during the experimental period in the mice treatment. Error bars are based on the standard deviations (SD) of 4 mice.

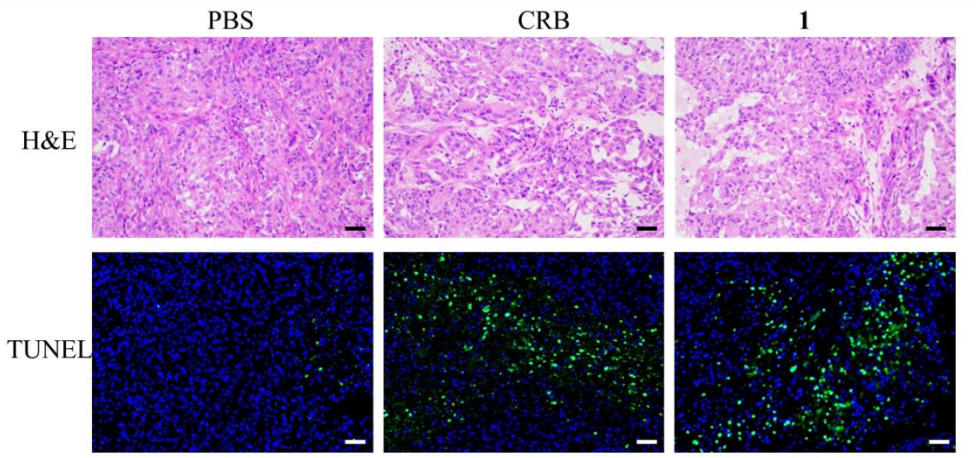

Figure S29. H&E and TUNEL stained tumor slices after various treatments, Related to STAR Methods. TUNEL-stained cell nuclei were stained with DAPI (blue fluorescence). Green fluorescence indicates TUNEL-positive cells. Scale bar =50 μm.

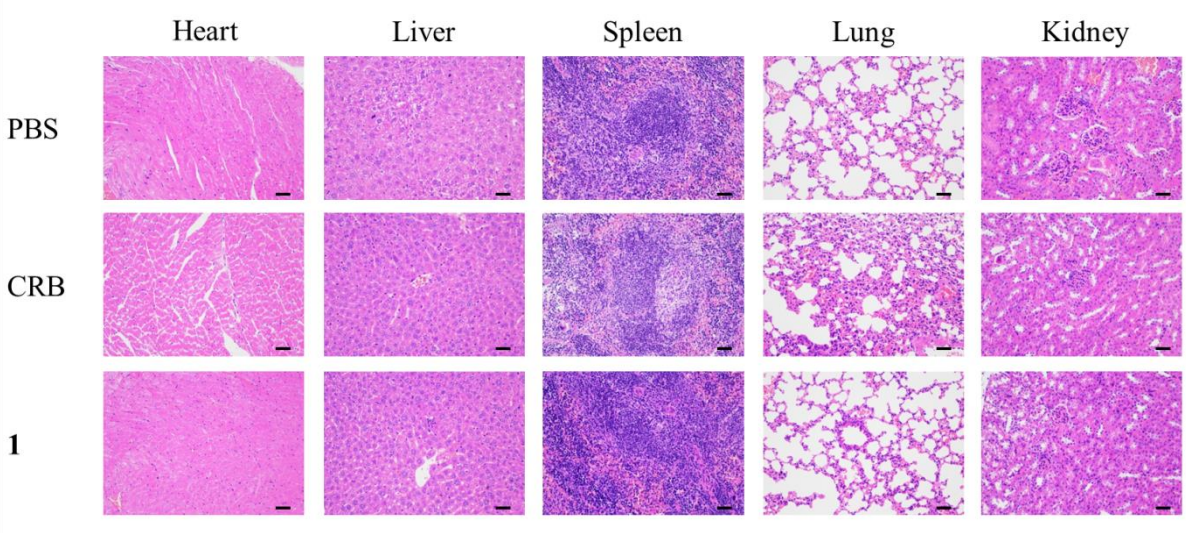

Figure S30. H&E-stained tissue sections from the heart, liver, spleen, lung, and kidney of the A549-tumor-bearing BALB/c nude mice after different treatments, Related to STAR Methods. Scale bar=50 μm**.**

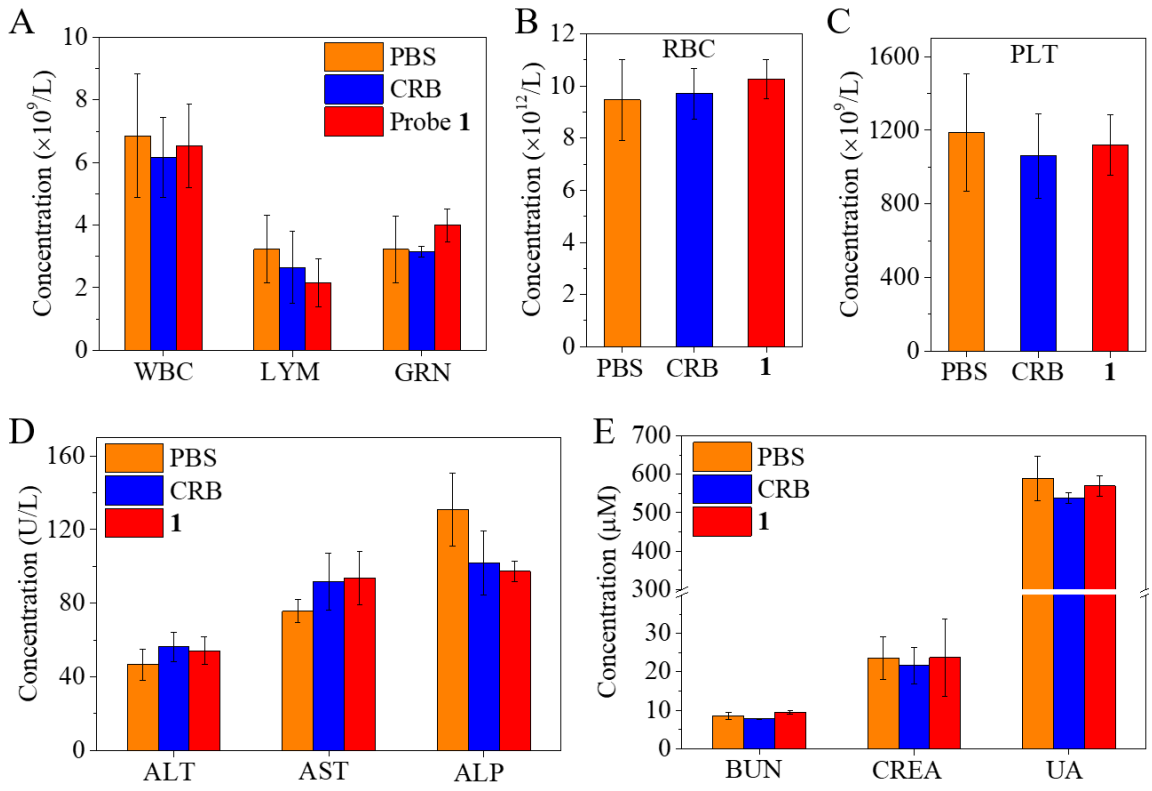

Figure S31. Hematology analysis of mice with different treatments, Related to STAR Methods. Error bars are based on the standard deviations (SD) of 4 mice.

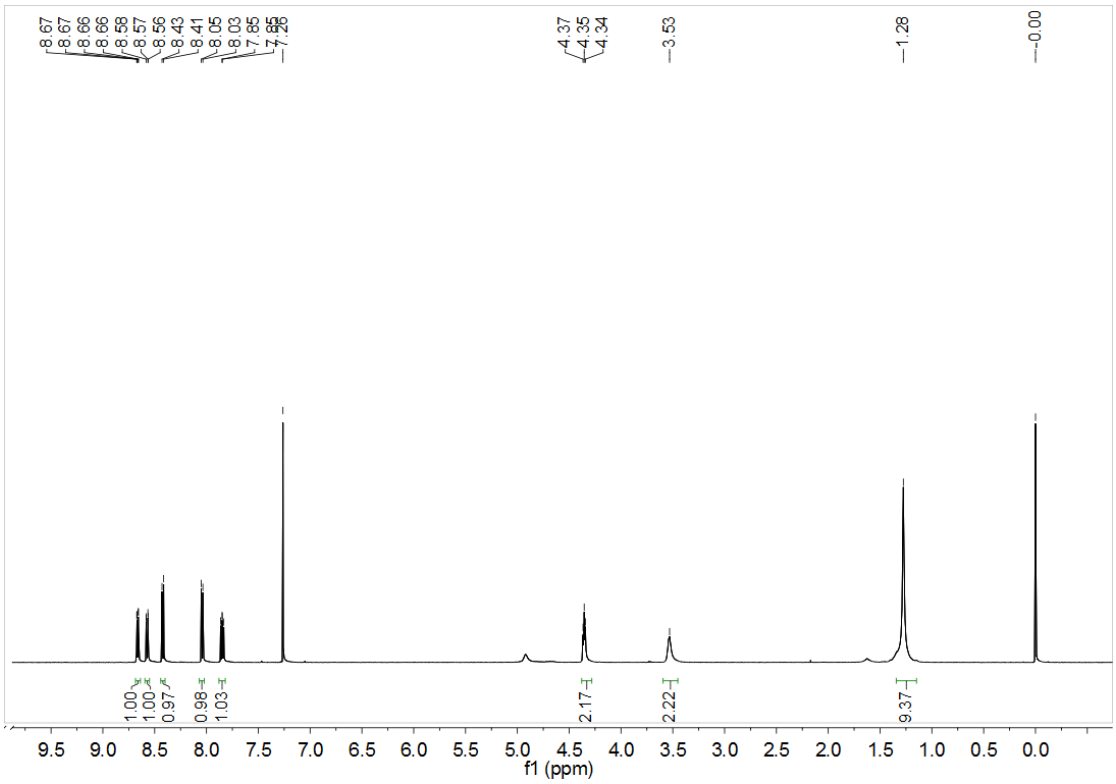

Figure S32. ^{1}H NMR spectra of compound 3 record in $CDCl_3$, Related to STAR Methods.

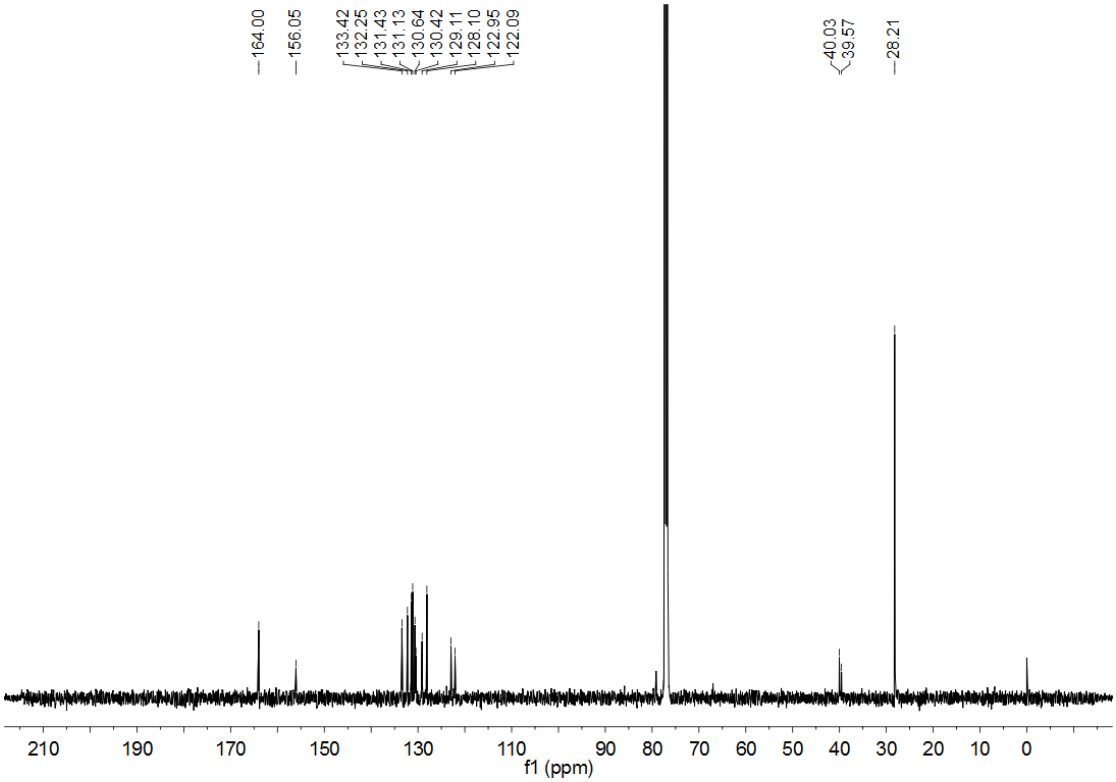

Figure S33. ^{13}C NMR spectra of compound 3 record in $CDCl_3$, Related to STAR Methods.

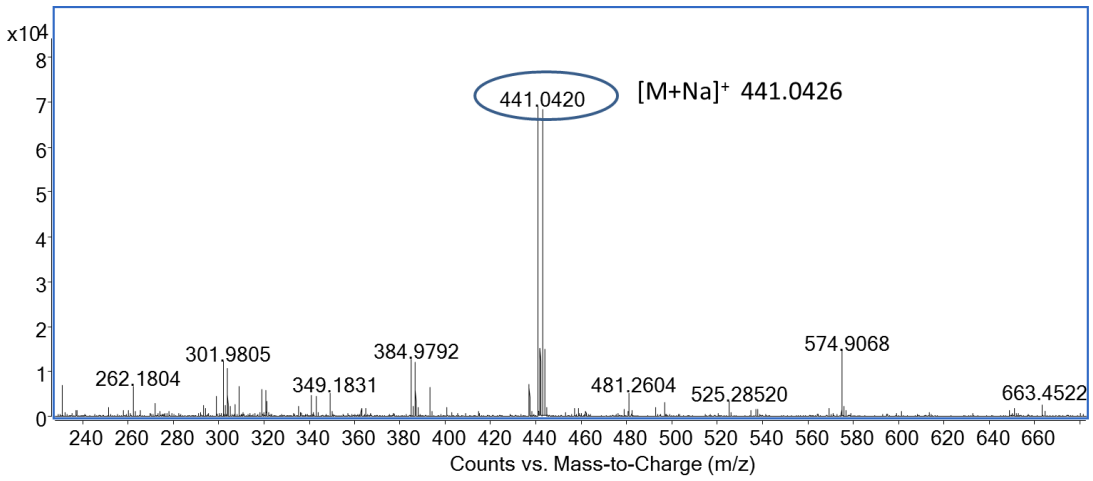

Figure S34. ESI-HRMS spectra of compound 3, Related to STAR Methods.

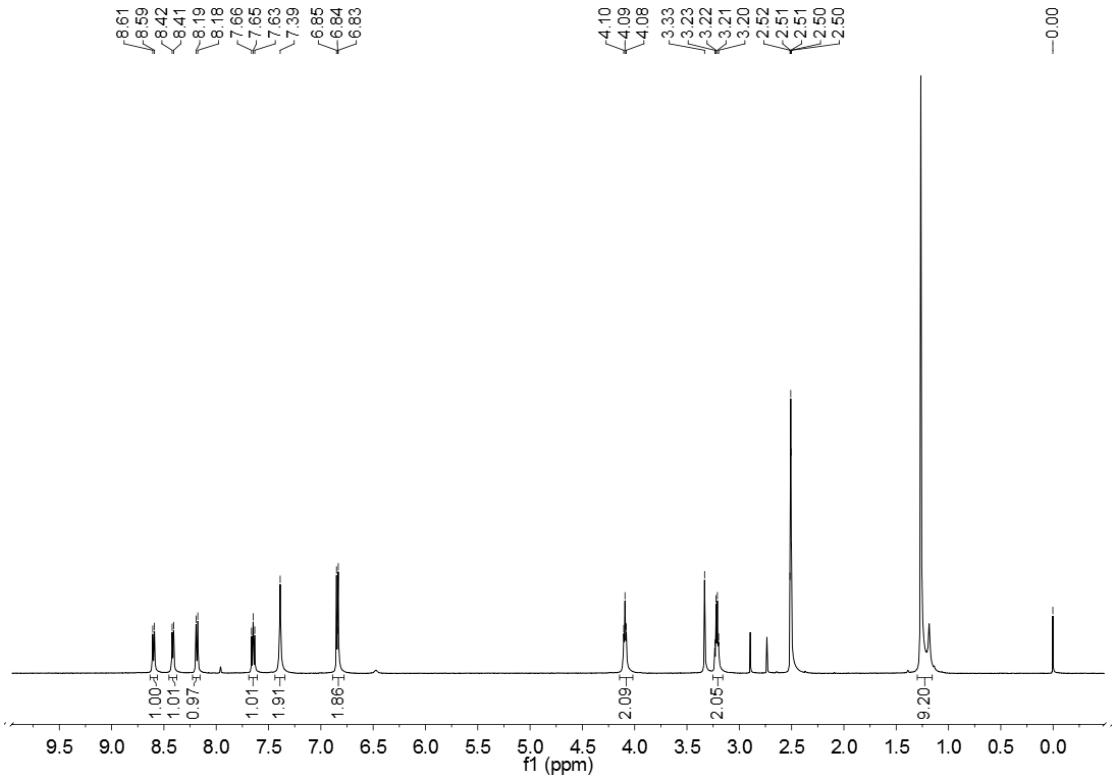

Figure S35. ^{1}H NMR spectra of compound 5 record in DMSO-d6, Related to STAR Methods.

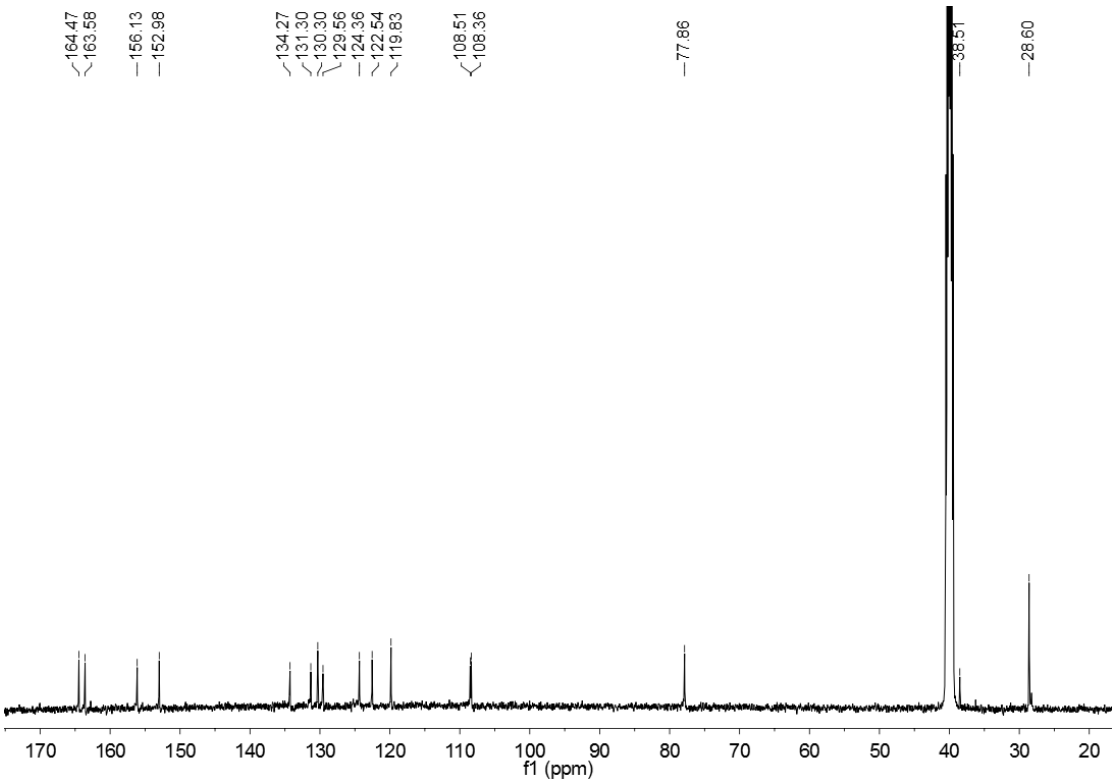

Figure S36. ^{13}C NMR spectra of compound 5 record in DMSO-d6, Related to STAR Methods.

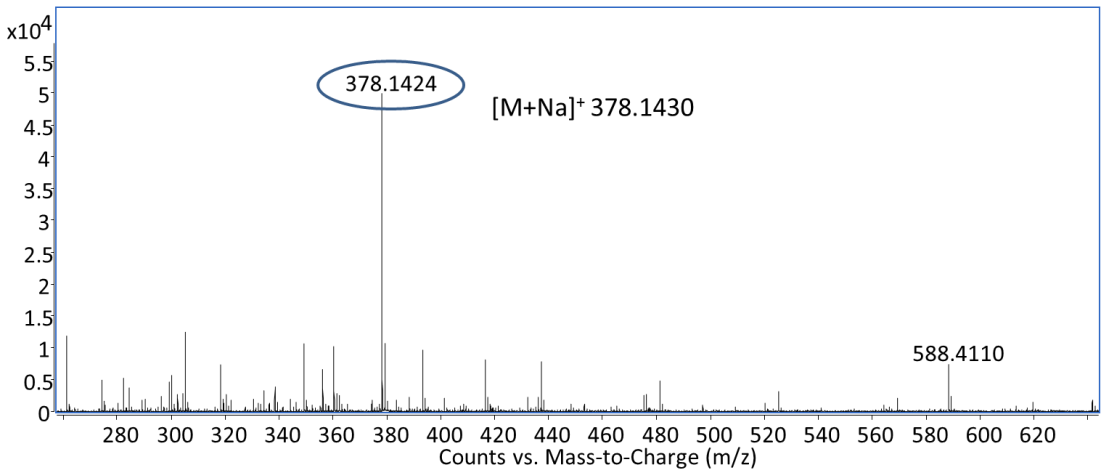

Figure S37. ESI-HRMS spectra of compound 5, Related to STAR Methods.

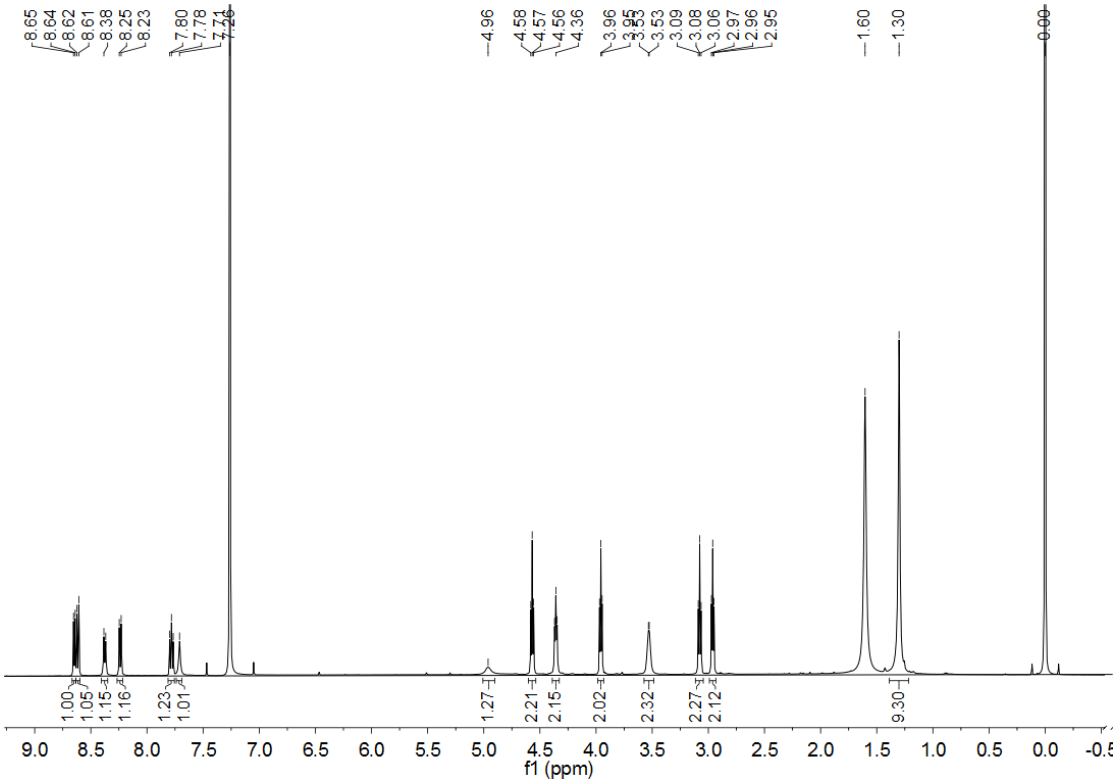

Figure S38. ^{1}H NMR spectra of compound 6 record in $CDCl_3$, Related to STAR Methods.

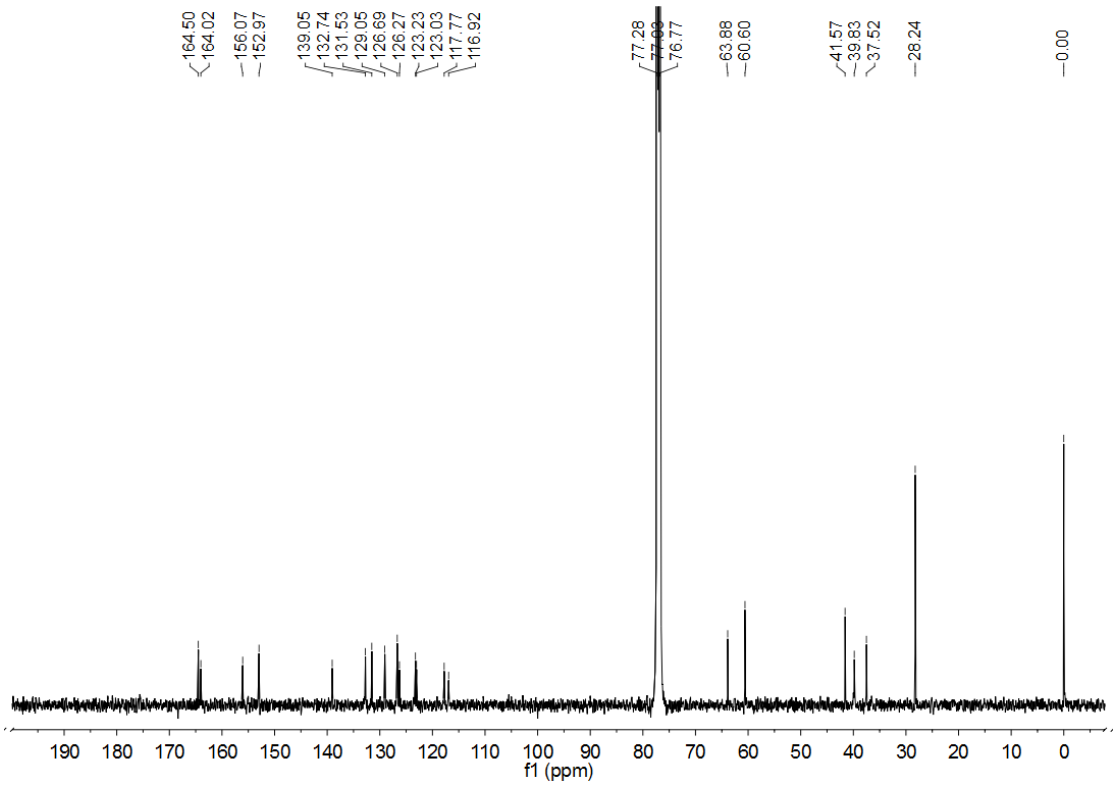

Figure S39. ^{13}C NMR spectra of compound 6 record in $CDCl_3$, Related to STAR Methods.

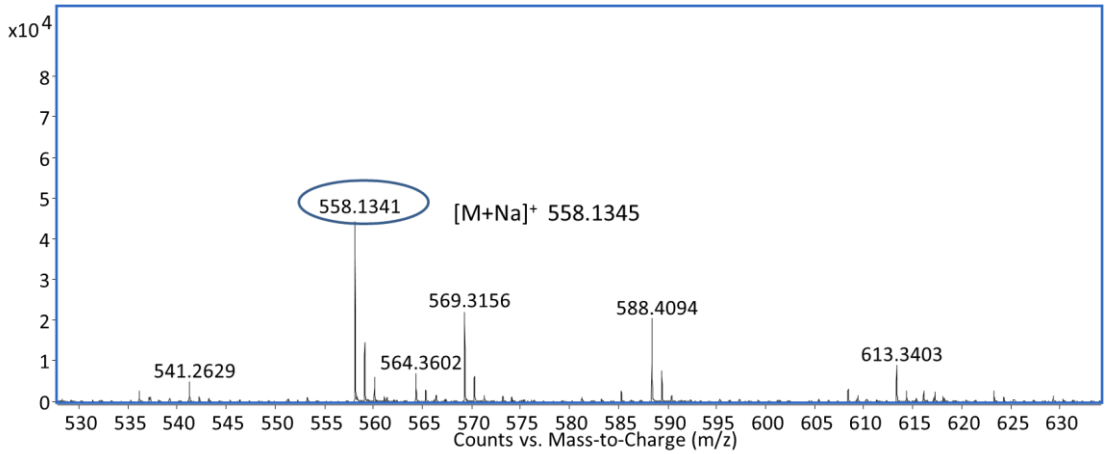

Figure S40. ESI-HRMS spectra of compound 6, Related to STAR Methods.

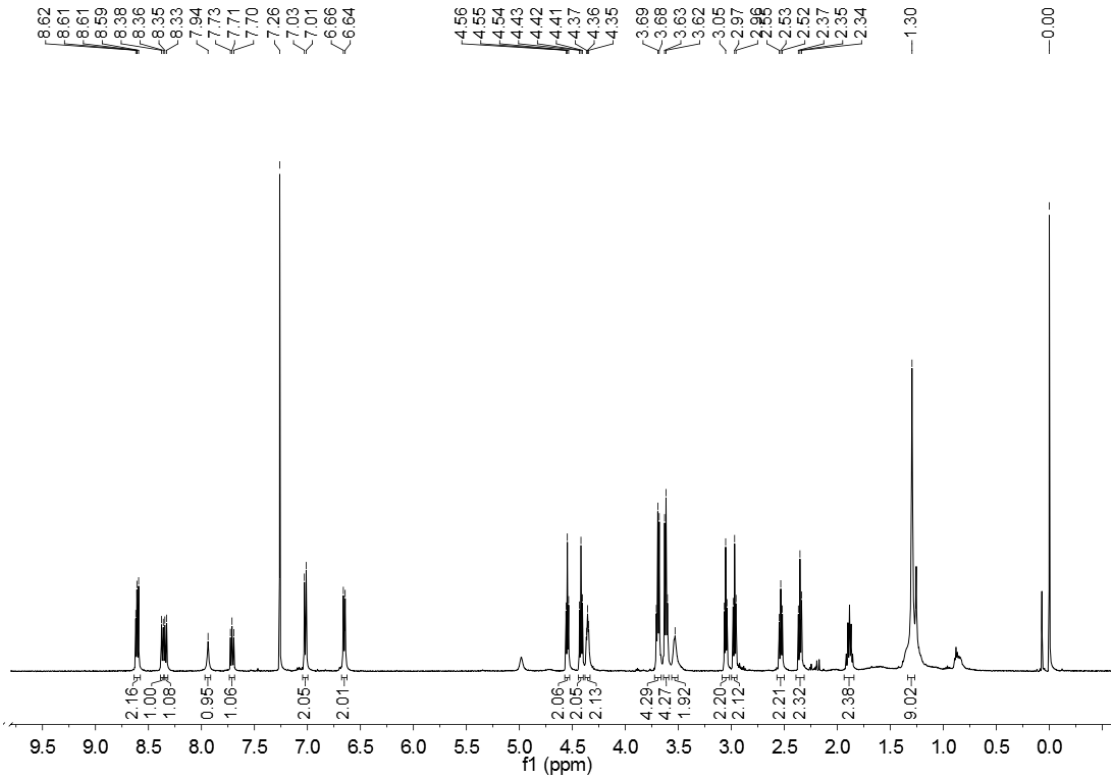

Figure S41. ^{1}H NMR spectra of compound 7 record in $CDCl_3$, Related to STAR Methods.

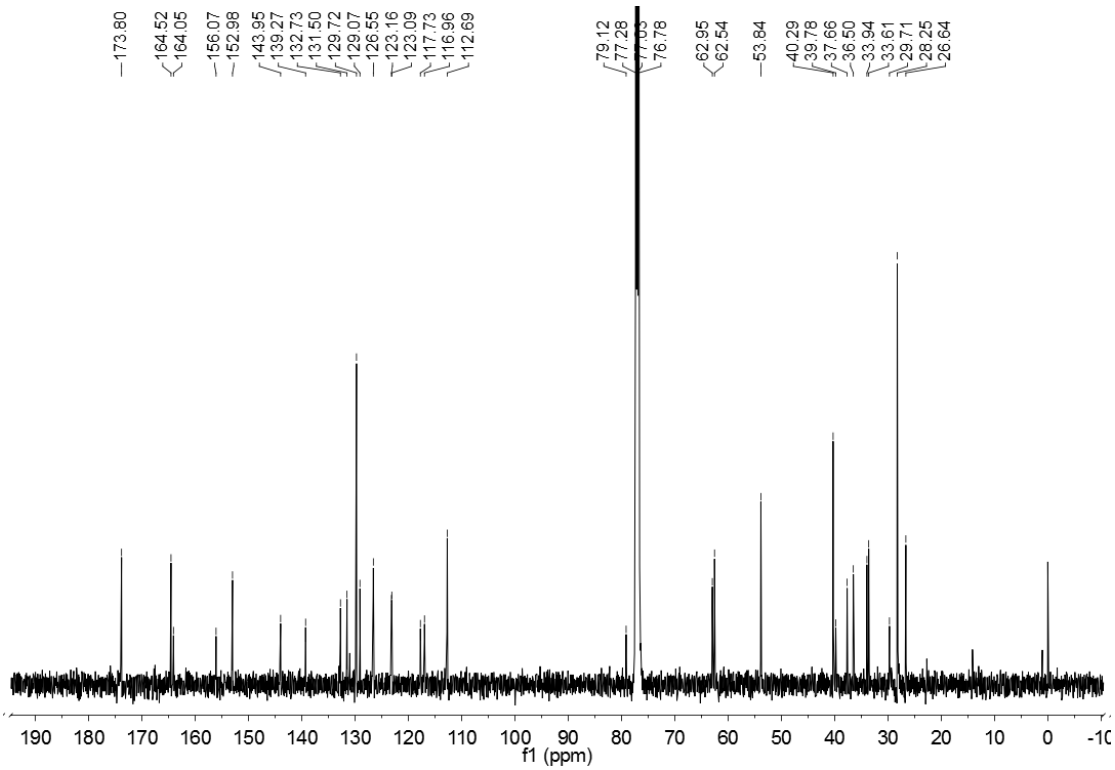

Figure S42. ^{13}C NMR spectra of compound 7 record in $CDCl_3$, Related to STAR Methods.

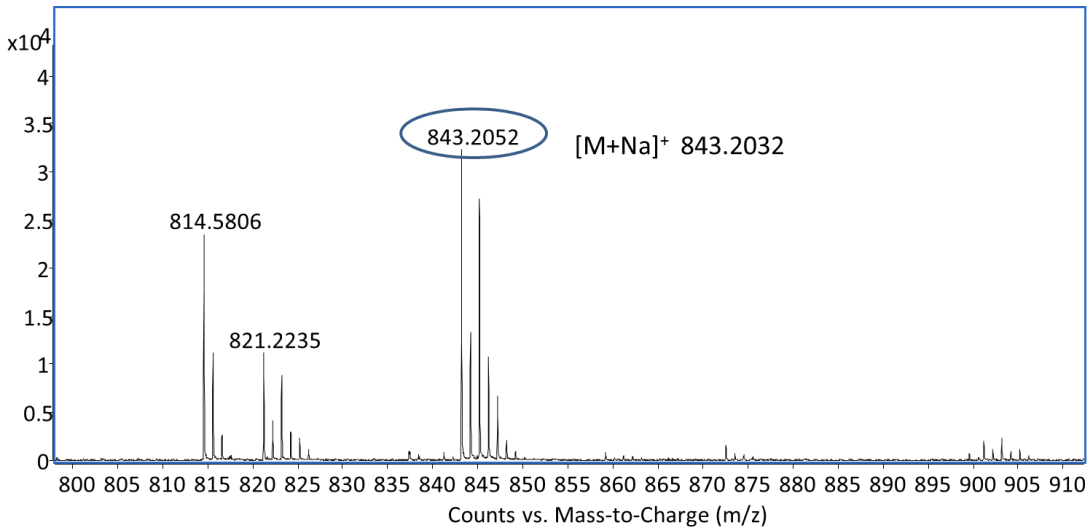

Figure S43. ESI-HRMS spectra of compound 7, Related to STAR Methods.

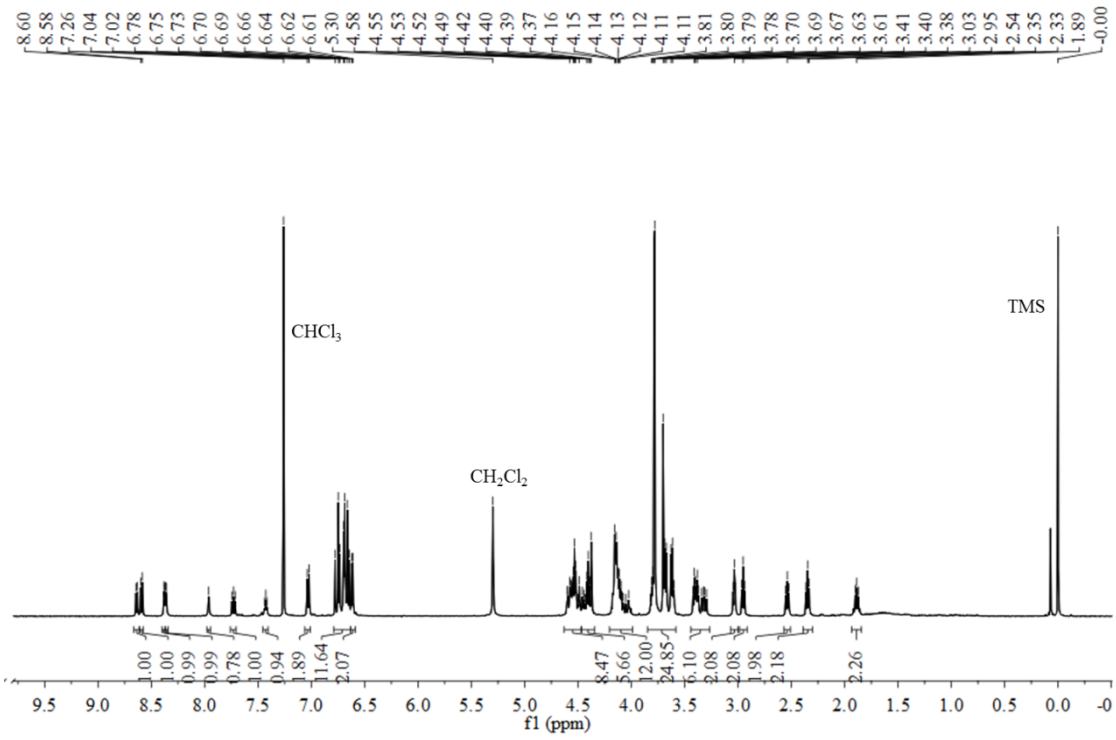

Figure S44. ^{1}H NMR spectra of Molego 1 record in $CDCl_3$, Related to STAR Methods.

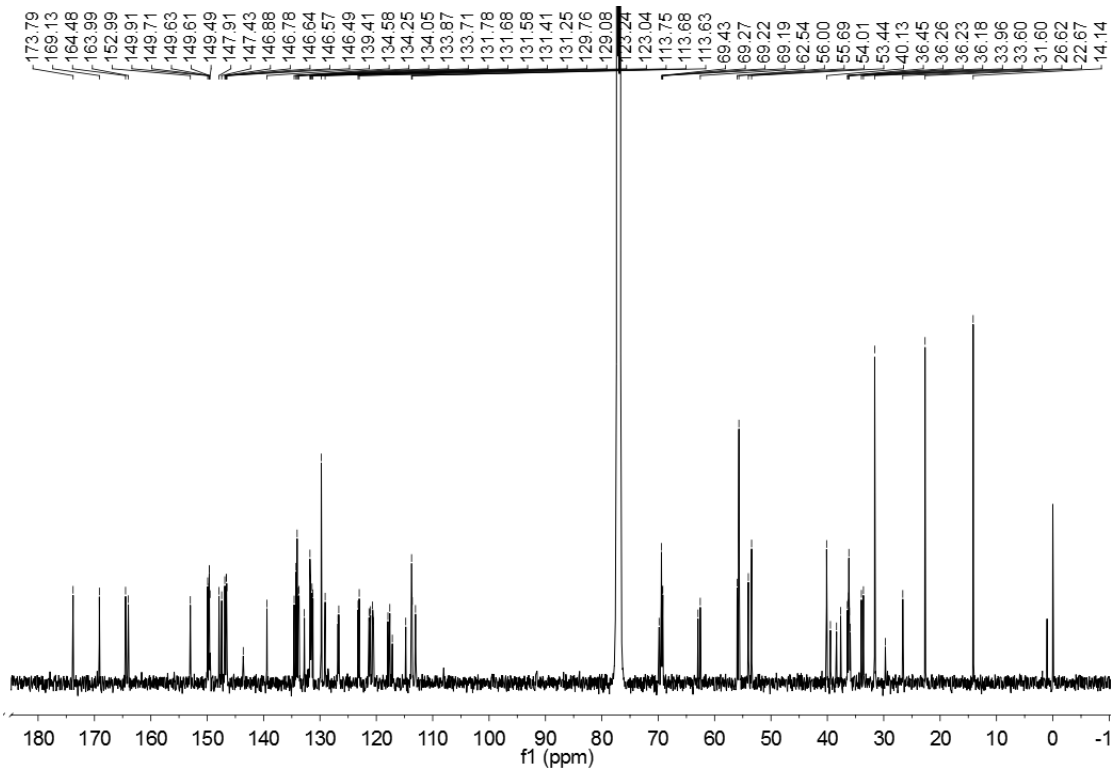

Figure S45. ^{13}C NMR spectra of Molego 1 record in $CDCl_3$, Related to STAR Methods.

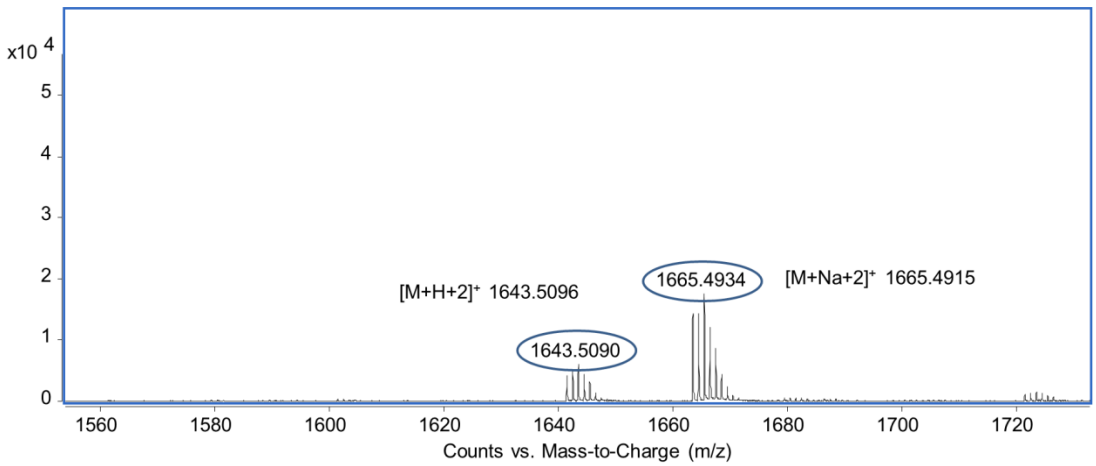

Figure S46. ESI-HRMS spectra of Molego 1, Related to STAR Methods.

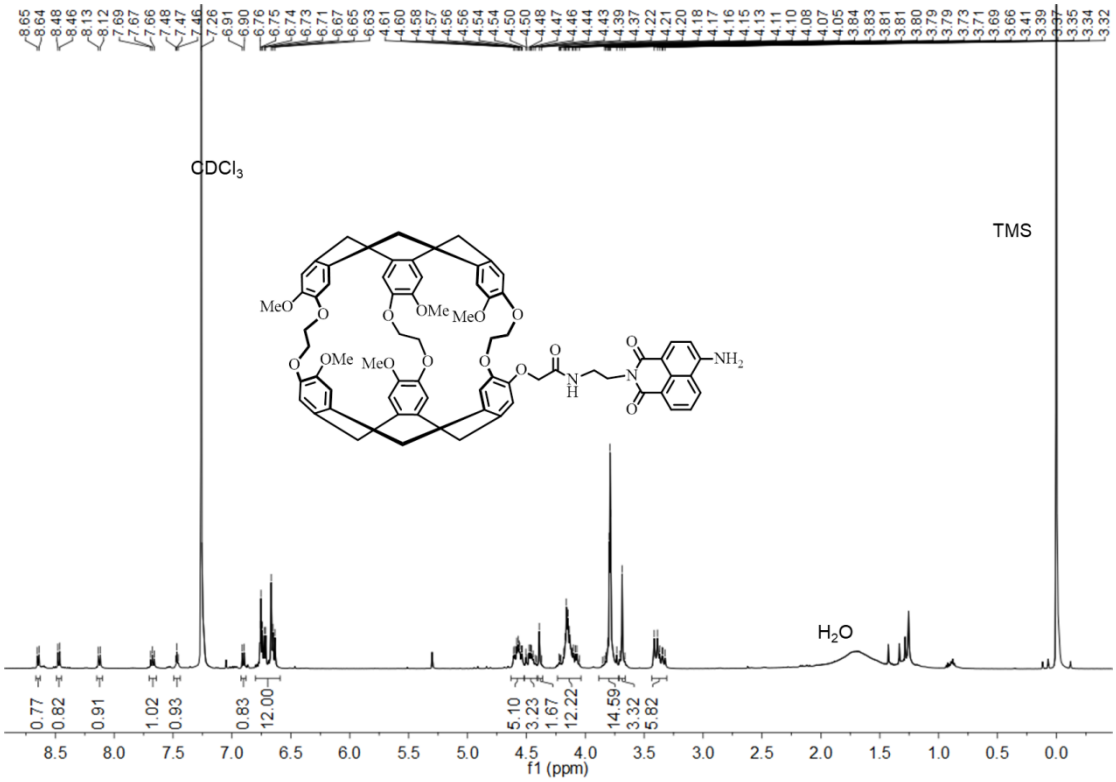

Figure S47. ^{1}H NMR spectra of compound 2 record in $CDCl_3$, Related to STAR Methods.

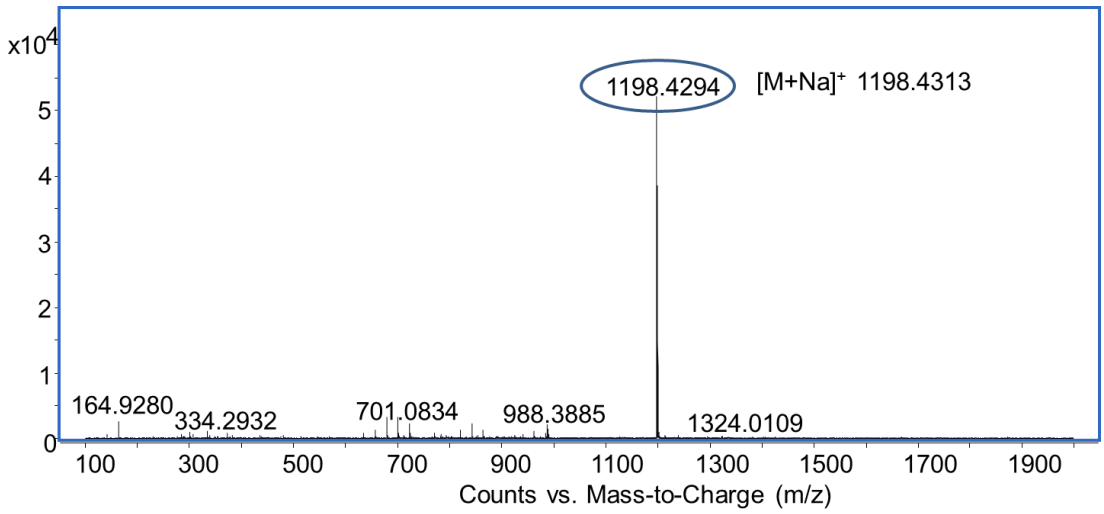

Figure S48. ESI-HRMS spectra of compound 2, Related to STAR Methods.